SMEFT projections at the EIC and LHeC to NLO QCD

Candidacy Talk

Kağan Şimşek

Committee members:

John Joseph Carrasco

André de Gouvêa

Frank Petriello (advisor, chair)

December 2, 2022

Outline

Prelude

- We study PVDIS asymmetries in NC cross sections at the EIC and NC DIS cross sections at the LHeC.
- BSM effects are parametrized in the model-independent SMEFT framework.
- Higher-dimensional operators are built using the existing SM particles with Wilson coefficients introduced as effective couplings at a UV scale Λ:

$$\mathscr{L}_{\text{SMEFT}} = \mathscr{L}_{\text{SM}} + \sum_{n>4} \frac{1}{\Lambda^{n-4}} \sum_{k} C_k^{(n)} O_k^{(n)}$$

- All new physics is assumed to be heavier than all the SM states and well beyond accessible collider energy.
- We focus on SMEFT corrections to the ffV vertices, as well as semi-leptonic 4-fermion operators at $n = 6$.

We find that

- the EIC can probe complementarily and competitively to the LHC NC Drell-Yan, resolving blind spots observed;
- the EIC can barely compete with the LHeC; nonetheless, they yield distinct correlations, showing complementarity;
- flat directions observed in the fit one LHeC run can be resolved by other runs and even by the EIC; and
- the LHeC seems promising in resolving flat directions in the ffV sector observed in the EW pole-observable (EWPO) fits.

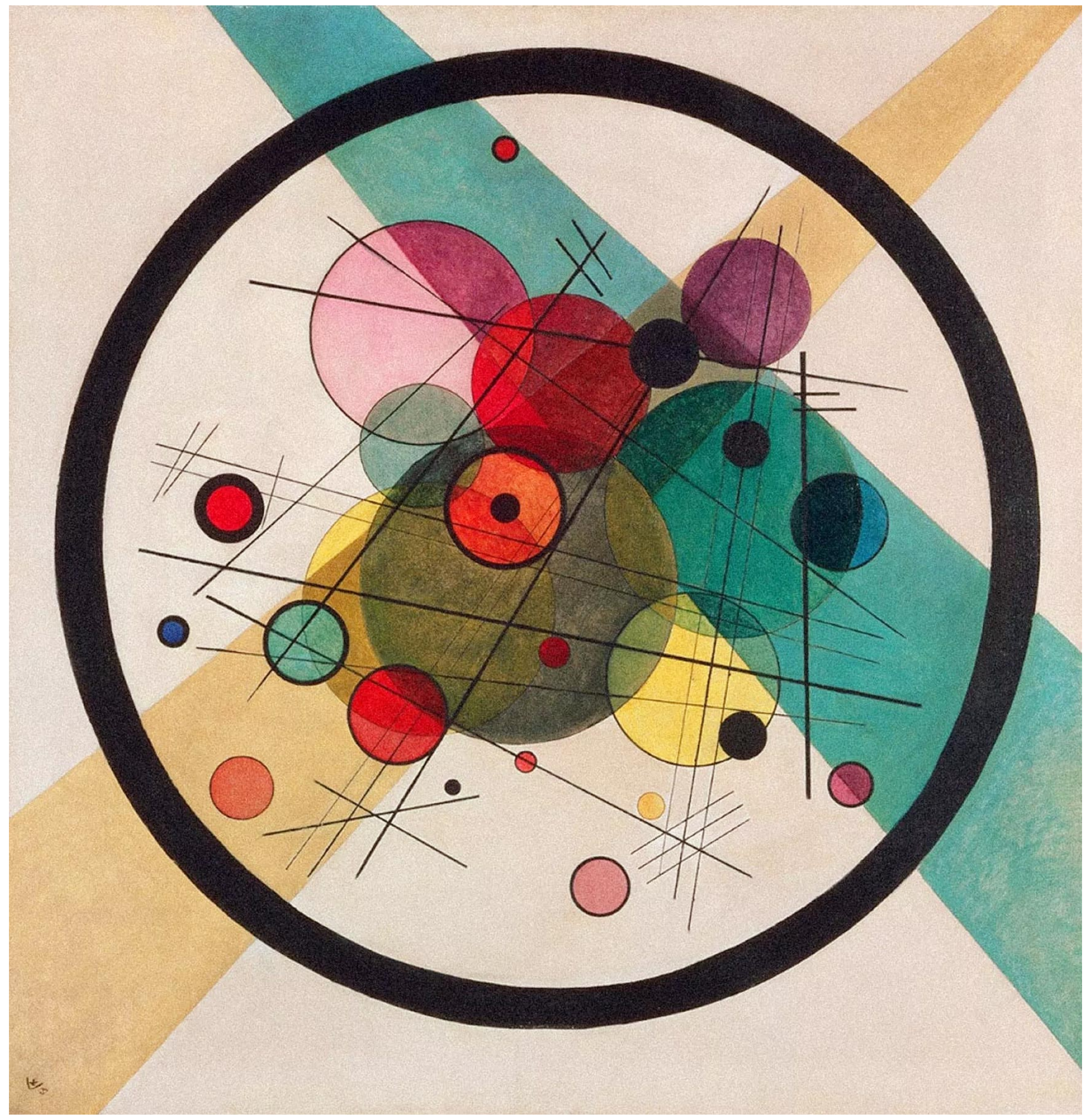

EIC and LHeC

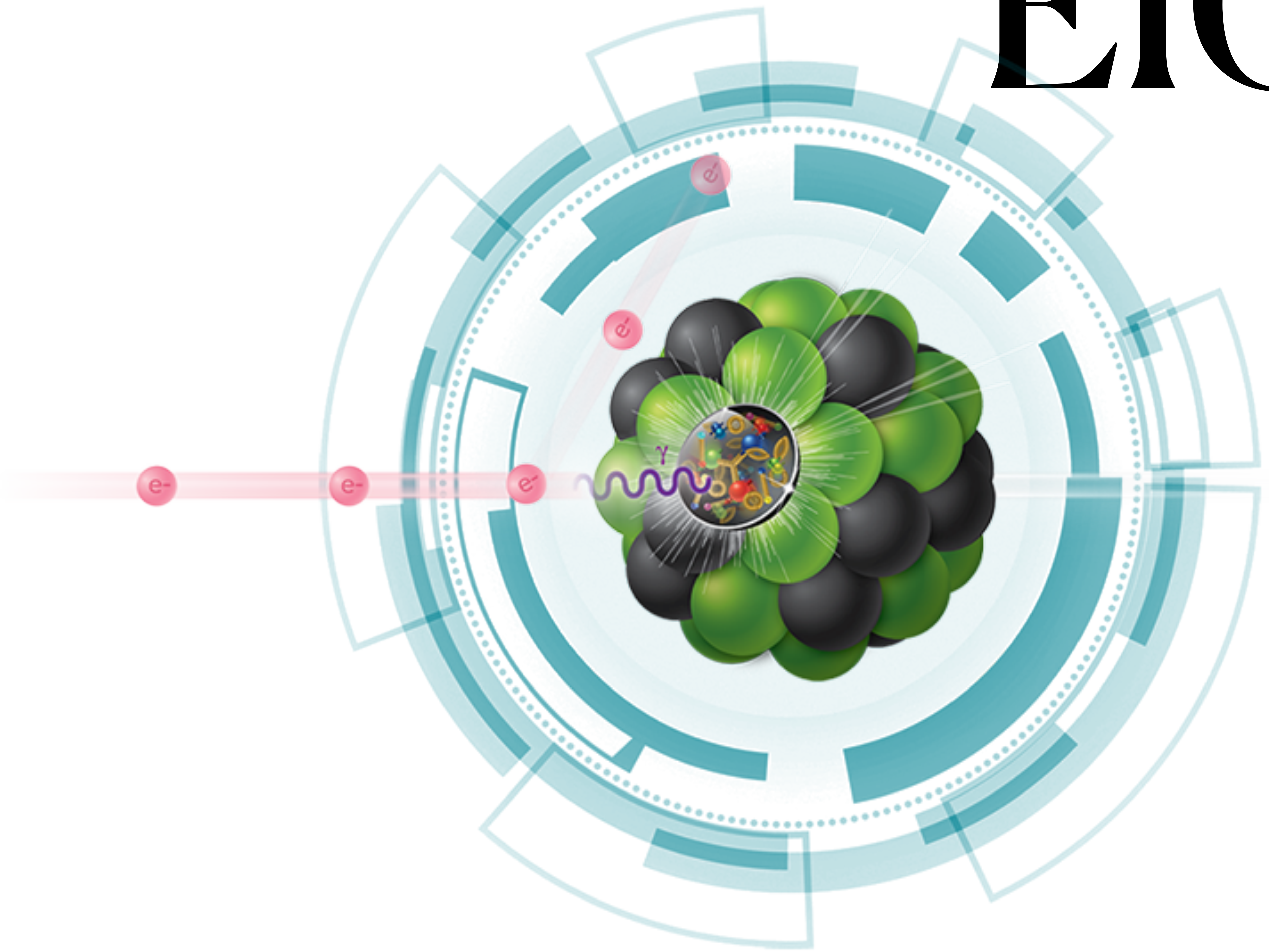

Next-gen electron-hadron colliders: EIC and LHeC

Electron-hadron colliders: [Brüning *et al.* FPhy (2022)]

- Ultimate tool for high-precision QCD studies
- Ultimate microscope for probing internal structure of hadrons
- e^- is an ideal probe of proton structure due to unmatched precision of QED interaction:
  - Virtual photon and vector bosons probe proton structure in a clean environment
  - Kinematics is uniquely determined by e^- beam and scattered lepton
- *Hadron-Elektron-Ringanlage* (HERA @ DESY, Germany) was the only e^-H collider ever operated (1991-2007).
- Electron-Ion Collider (EIC) is currently under construction at BNL @ NY.
- Large Hadron-electron Collider (LHeC @ CERN, Switzerland) is awaiting approval.

EIC [Accardi *et al.* 1212.1701]

- A US DOE project under construction in Brookhaven National Laboratory, Upton, NY.
- It will use the Relativistic Heavy Ion Collider (RHIC @ BNL, in operation since 2000) accelerator complex. (RHIC is the first heavy-ion collider and also the world's only spin-polarized proton collider.)
- It will combine the experience from HERA to deliver polarized e^- beams with the experience from RHIC to be the first machine that provides the collision of polarized e^- with polarized p, and at a later stage, polarized ^{2}H and ^{3}He.
- It is planned to start operating in a decade.

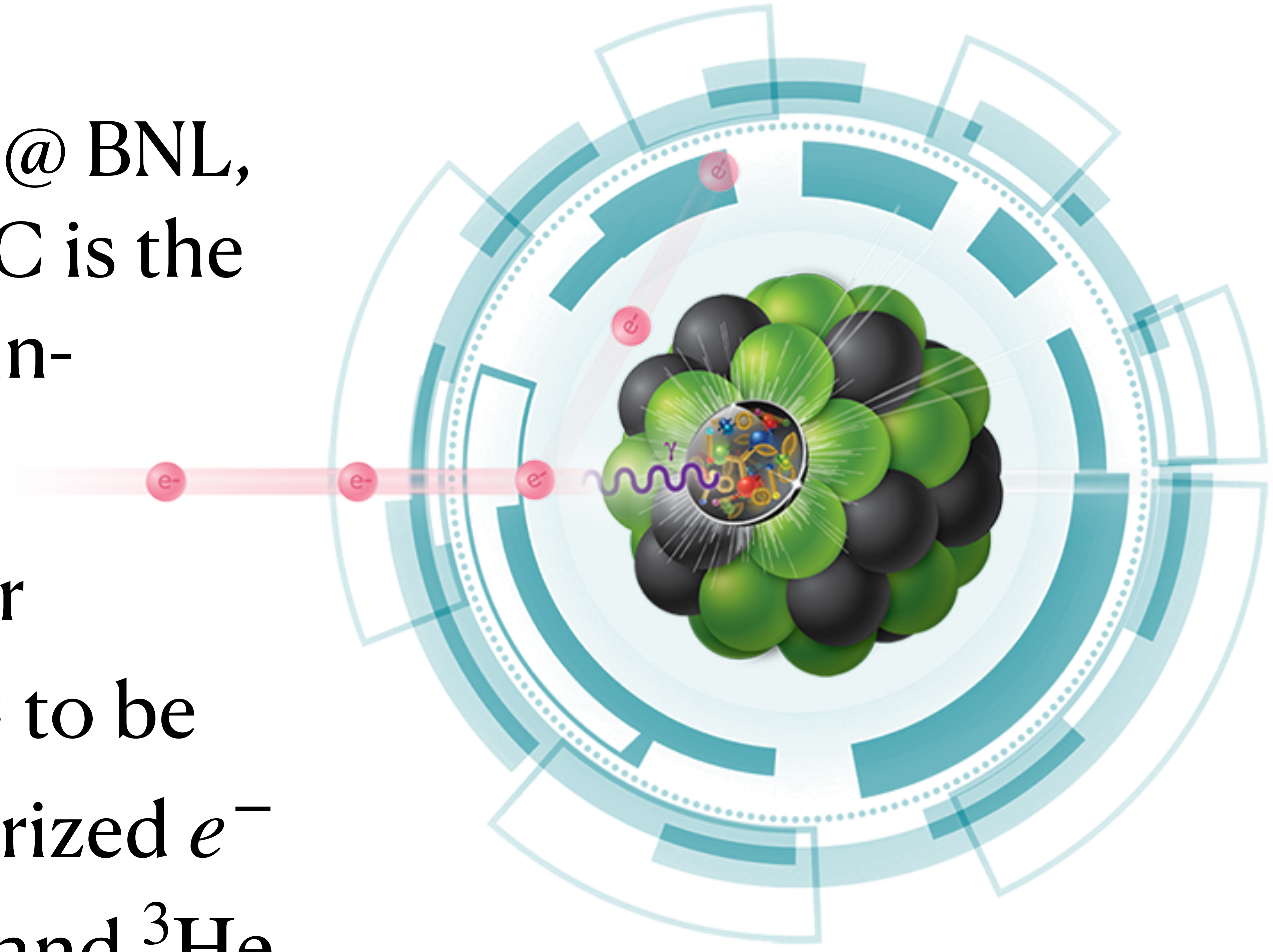

Image credit: bnl.gov

EIC [Accardi *et al.* 1212.1701]

Unique features:

- Designed to collide 5 to 18 GeV polarized e^- beams with 41 to 275 GeV polarized p beams, polarized light ions with energies up to 166 GeV (^{3}He), and unpolarized heavy ion beams up to 110 GeV.
- CM energies between fixed-target scattering and high-energy colliders, 70 to140 GeV
- First lepton-ion collider to polarize both beams
- First collider with fast spin-flip capacity

EIC [Accardi *et al.* 1212.1701]

From these unique features:

- Extraction of PVDIS asymmetries in EW NC cross section
- Reduced uncertainties from luminosity and detector acceptance/efficiency
- Explore issues in QCD
- Probes of BSM physics

Also a positron beam in the future to study electron-positron (lepton-charge) asymmetries.

LHeC [Fernandez *et al.* 1206.2913]

- 1984: Idea of an $e^{-}p$ collider in the LEP-LHC tunnel was first discussed (around the same time HERA was approved).
- 2005: It was found feasible to simultaneously operate pp in the LHC and ep in the new machine termed LHeC, which would be complementary to the LHC (just as HERA was to Tevatron). Integrated luminosity was projected to be $O(100)\ \mathrm{fb}^{-1}$, a factor of 100 more than HERA had collected over its lifetime of 15 years.
- Center of mass energies of $\sqrt{s} \simeq 1.5\ \mathrm{TeV}$ for DIS measurements:
  - Searches and analysis for BSM physics
  - Novel measurements in QCD
  - EW physics to unprecedented precision
  - DIS physics at low Bjorken x
- Suggested electron beam energies: 50 to $150\ \mathrm{GeV}$; the chosen default value is $60\ \mathrm{GeV}$.

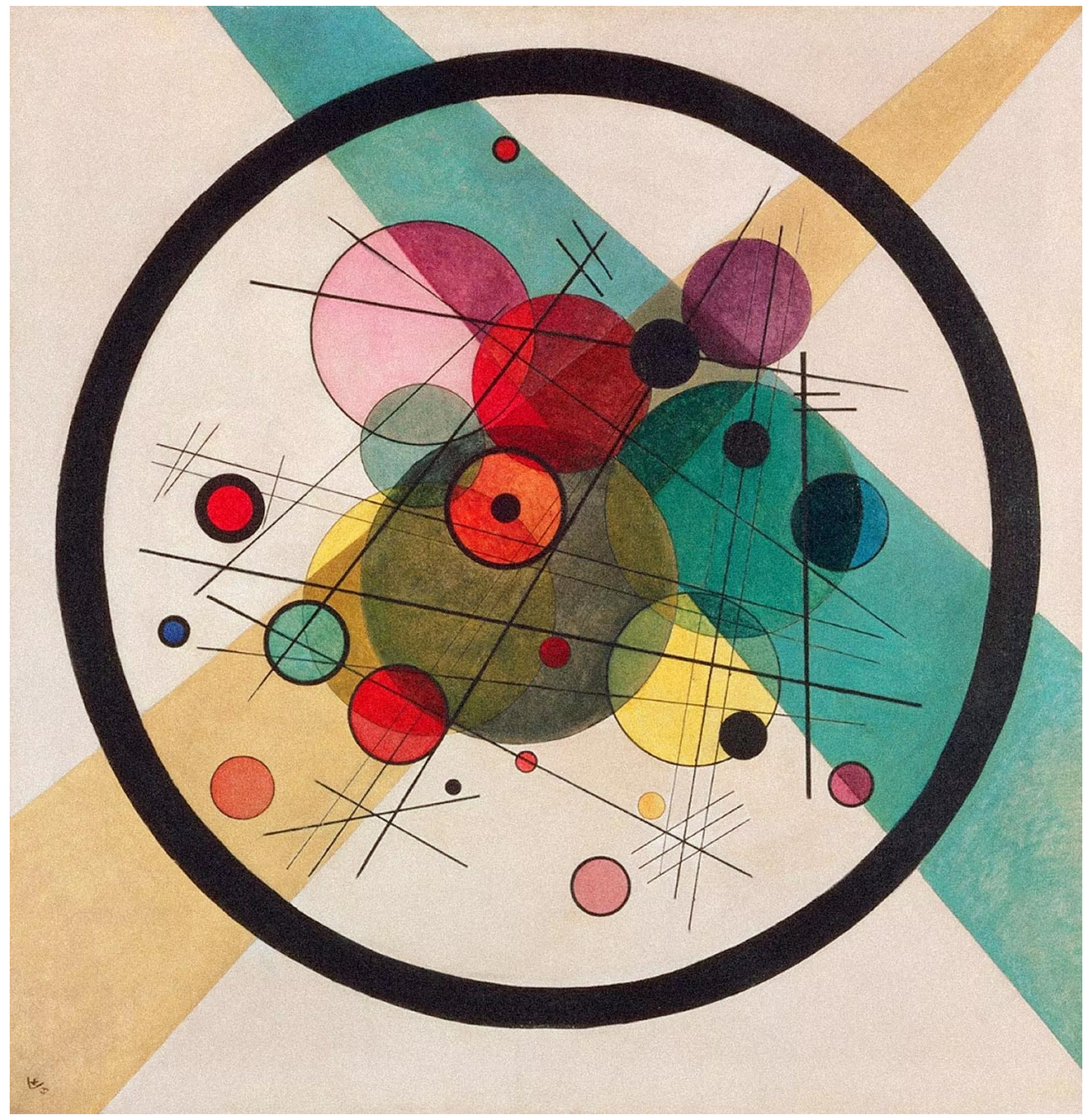
W. Kandinsky, *Circles in a* circle.
Image credit: wassilykandinsky.net

LHeC [Fernandez *et al.* 1206.2913]

- 2011: First complete draft of conceptual design of the LHeC
- The LHeC will be an upgrade of the LHC.
  - Substantially enriches the physics harvest related to huge investment in the LHC
  - An e^-p collider operating at an energy frontier
  - *Guaranteed* to deepen the understanding of TeV-scale physics
- The LHeC needs the LHC proton/ion beams ⇒ synchronous pp and e^-p operation, as well as HH and e^-H, including deuterons.
- The earliest realistic operational period coincides with the LHC Run 5 period in 2032.

Review of the SMEFT

Standard Model Effective Field Theory:

- A model-independent extension to the Standard Model.
- Operators of dimensions higher than 4 built of the existing spectrum of SM.
- Wilson coefficients as effective couplings at UV scale Λ beyond accessible collider energies:

$$\mathscr{L}_{\text{SMEFT}} = \mathscr{L}_{\text{SM}} + \sum_{n>4} \frac{1}{\Lambda^{n-4}} \sum_{k} C_k^{(n)} O_k^{(n)}$$

- Focus on $n = 6$.
- Consider only SM-SMEFT interference in cross sections for consistency.

16 operators affecting DIS at leading order in the *Warsaw* basis [Misiak *et al.* 1008.4884]:

- Modifying ffV vertices in a nonuniversal manner:

$$O_{\varphi\ell}^{(1)} = (\varphi^\dagger i \overleftrightarrow{D}_\mu \varphi)(\bar{\ell}\gamma^\mu \ell)$$

$$O_{\varphi\ell}^{(3)} = (\varphi^\dagger i \overleftrightarrow{D}_\mu \tau^I \varphi)(\bar{\ell}\gamma^\mu \tau^I \ell)$$

$$O_{\varphi e} = (\varphi^\dagger i \overleftrightarrow{D}_\mu \varphi)(\bar{e}\gamma^\mu e)$$

$$O_{\varphi q}^{(1)} = (\varphi^\dagger i \overleftrightarrow{D}_\mu \varphi)(\bar{q}\gamma^\mu q)$$

$$O_{\varphi q}^{(3)} = (\varphi^\dagger i \overleftrightarrow{D}_\mu \varphi)(\bar{q}\gamma^\mu \tau^I q)$$

$$O_{\varphi u} = (\varphi^\dagger i \overleftrightarrow{D}_\mu \varphi)(\bar{u}\gamma^\mu \tau^I u)$$

$$O_{\varphi d} = (\varphi^\dagger i \overleftrightarrow{D}_\mu \varphi)(\bar{d}\gamma^\mu d)$$

- Modifying ffV vertices in a universal manner:

$$O_{\varphi WB} = (\varphi^\dagger \tau^I \varphi) W_{\mu\nu}^I B^{\mu\nu}$$

$$O_{\varphi D} = (\varphi^\dagger D_\mu \varphi)^* (\varphi^\dagger D^\mu \varphi)$$

$$\varphi^\dagger i \overleftrightarrow{D}_\mu \varphi = \varphi^\dagger i D_\mu \varphi + \mathrm{h.c.}$$

$$\varphi^\dagger i \overleftrightarrow{D}_\mu \tau^I \varphi = \varphi^\dagger i D_\mu \tau^I \varphi + \mathrm{h.c.}$$

- Inducing semi-leptonic 4-fermion interaction:

$$O_{eu} = (\bar{e}\gamma_\mu e)(\bar{u}\gamma^\mu u)$$

$$O_{ed} = (\bar{e}\gamma_\mu e)(\bar{d}\gamma^\mu d)$$

$$O_{\ell q}^{(1)} = (\bar{\ell}\gamma_\mu \ell)(\bar{q}\gamma^\mu q)$$

$$O_{\ell q}^{(3)} = (\bar{\ell}\gamma_\mu \tau^I \ell)(\bar{q}\gamma^\mu \tau^I q)$$

$$O_{\ell u} = (\bar{\ell}\gamma_\mu \ell)(\bar{u}\gamma^\mu u)$$

$$O_{\ell d} = (\bar{\ell}\gamma_\mu \ell)(\bar{d}\gamma^\mu d)$$

$$O_{qe} = (\bar{e}\gamma_\mu e)(\bar{q}\gamma^\mu q)$$

Review of the DIS formalism

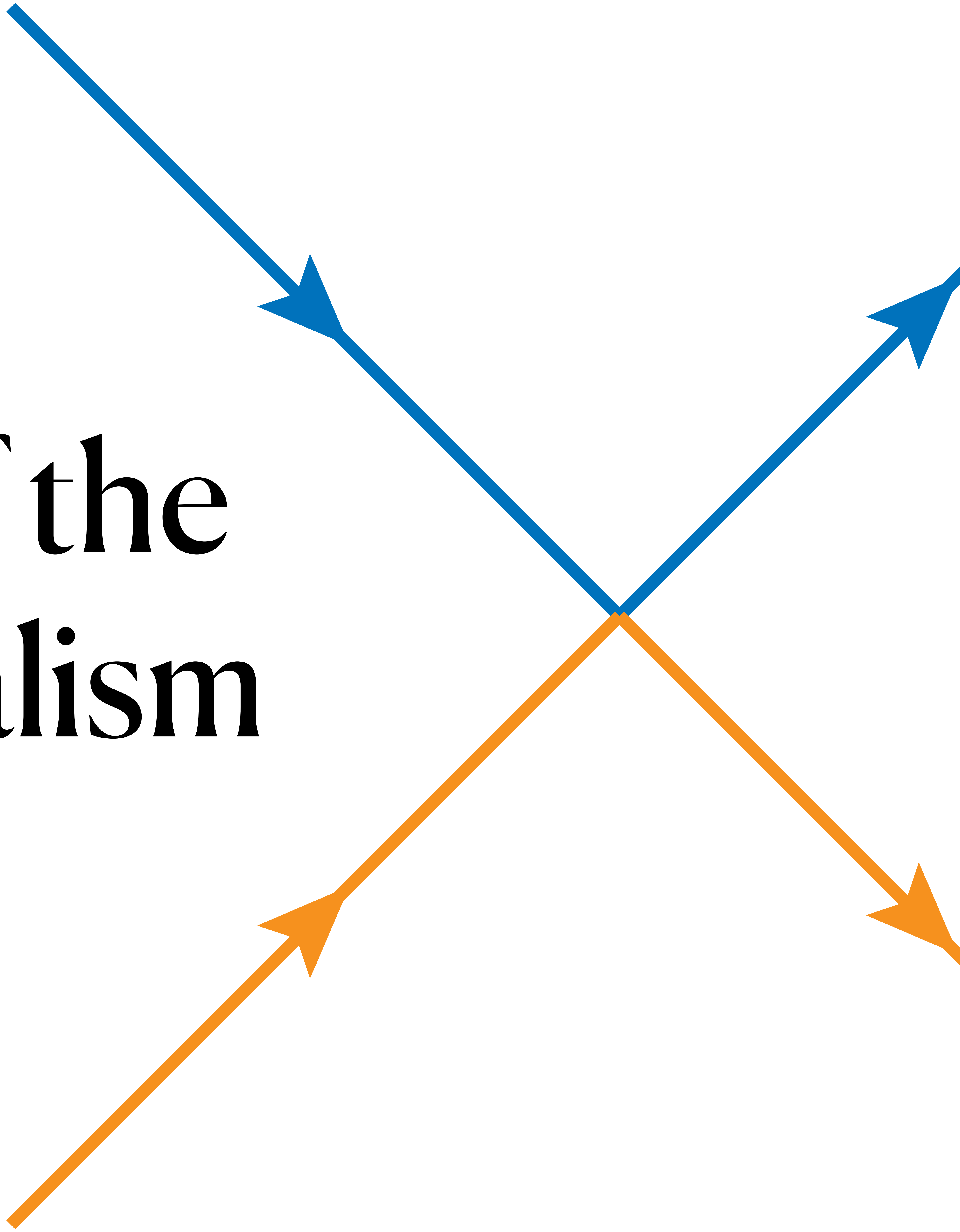

DIS cross section at LO

NC DIS in the process $\ell(k) + H(P) \to \ell'(k') + X$, where ℓ is $e^{\pm}$, H is p or D.

LO partonic process: $\ell(k) + q(p) \to \ell'(k') + q'(p')$

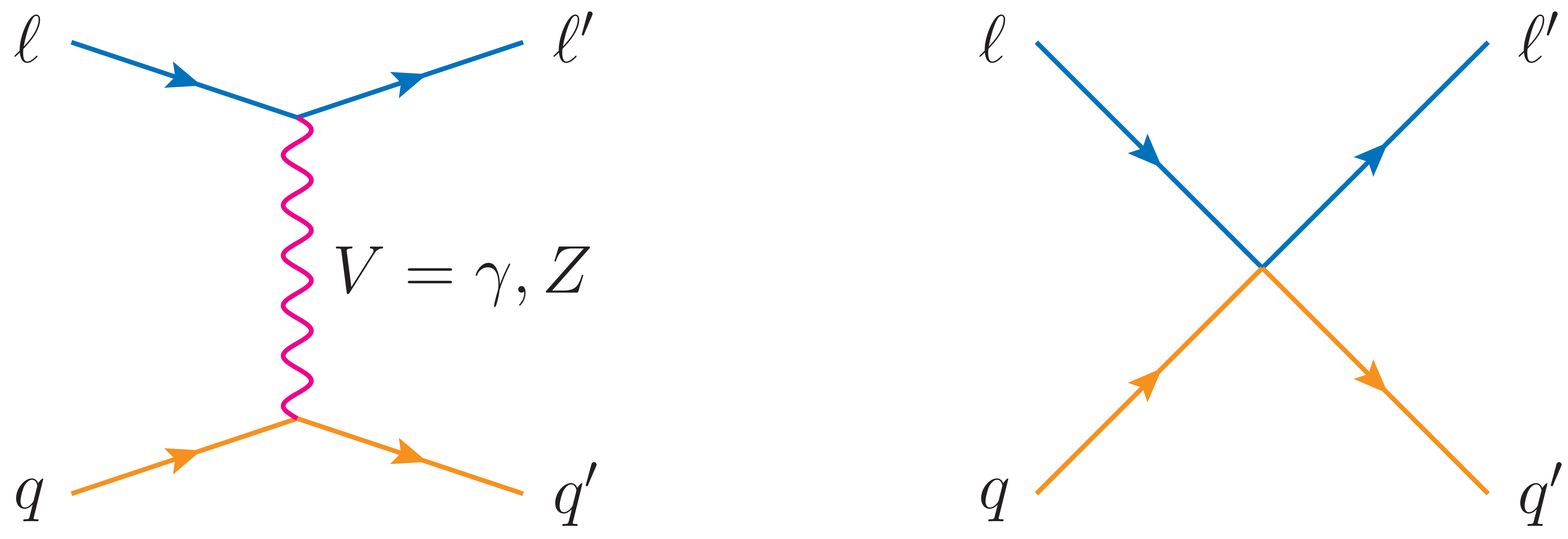

Possible gluon-initiated contact interaction: $\ell(k) + g(p) \to \ell'(k') + g'(p')$, but operators do not show up below dimension 8.

Parametrization of ffV and $\ell\ell qq$ vertex factors in $V - A$ basis:

$$V_{fV}^{V,A} = iC_V Q_{fV}^{V,A}, \qquad V_{\times q}^{PP'} = iC_{\times q}^{PP'}$$

quantum numbers

strength of couplings

where

- $V = \gamma, Z, \times$ in subscript
- $V\,(A)$ means *vector* (*axial*) in superscript
- $P, P' = V, A$ indicates structure of lepton and quark currents at the contact point (e.g. $C_{\times q}^{VA}$ for coupling of $\bar{\ell}\gamma_\mu\ell$ and $\bar{q}\gamma^\mu\gamma_5 q$)
- all BSM effects are contained in $Q_{fV}^{V,A}$ for generalization to higher dimensions

Propagator:

$$P_V = \frac{1}{Q^2 + M_V^2}$$

Coupling strengths:

$$C_\gamma = -e = -\sqrt{4\pi\alpha}$$

$$C_Z = -g_Z = -\frac{e}{2c_W s_W} = -\sqrt{\sqrt{2}G_F M_Z^2}$$

$$C_{\times q}^{VV} = \frac{C_{eu/d} + (C_{\ell q}^{(1)} \mp C_{\ell q}^{(3)}) + C_{\ell u/d} + C_{qe}}{4\Lambda^2}$$

$$C_{\times q}^{VA} = \frac{C_{eu/d} - (C_{\ell q}^{(1)} \mp C_{\ell q}^{(3)}) + C_{\ell u/d} - C_{qe}}{4\Lambda^2}$$

$$C_{\times q}^{AV} = \frac{C_{eu/d} - (C_{\ell q}^{(1)} \mp C_{\ell q}^{(3)}) - C_{\ell u/d} + C_{qe}}{4\Lambda^2}$$

$$C_{\times q}^{AA} = \frac{C_{eu/d} + (C_{\ell q}^{(1)} \mp C_{\ell q}^{(3)}) - C_{\ell u/d} - C_{qe}}{4\Lambda^2}$$

Quantum numbers:

$$Q_{f\gamma}^V = Q_f + \mathcal{O}(C_k^2)$$

$$Q_{f\gamma}^A = 0$$

$$Q_{fZ}^V = g_V^f \left[1 + \frac{M_Z^2}{4\pi\alpha\Lambda^2} c_V^f(C_k^V, M_Z)\right]$$

$$Q_{fZ}^V = g_A^f \left[1 + \frac{M_Z^2}{4\pi\alpha\Lambda^2} c_A^f(C_k^A, M_Z)\right]$$

in the input basis $\{G_F, \alpha, M_Z\}$.

$C_k^{V,A} \in \{C_{\varphi WB}, C_{\varphi D}, C_{\varphi\ell}^{(1)}, C_{\varphi\ell}^{(3)}, C_{\varphi e}, C_{\varphi q}^{(1)}, C_{\varphi q}^{(3)}, C_{\varphi u}, C_{\varphi d}\}$

Relative couplings and propagators:

$$\eta_V = \frac{C_V^2 P_V}{C_\gamma^2 P_\gamma}, \qquad \eta_{\times q}^{PP'} = \frac{C_{\times q}^{PP'}}{C_\gamma^2 P_\gamma}$$

SMEFT LO structure functions:

$$F_1^{\widetilde{V}}(x, Q^2) = \frac{1}{2}\sum_q \lambda_V^{\widetilde{V}} q(x, Q^2)$$

$$g_1^{\widetilde{V}} = \frac{1}{2}\sum_q \lambda_V^{\widetilde{V}} \Delta q(x, Q^2)$$

$$F_3^{\widetilde{V}}(x, Q^2) = \sum_q - \mathrm{sgn}(q)\lambda_A^{\widetilde{V}} q(x, Q^2)$$

$$g_5^{\widetilde{V}}(x, Q^2) = \frac{1}{2}\sum_q \mathrm{sgn}(q)\lambda_A^{\widetilde{V}} \Delta q(x, Q^2)$$

$$F_L^{\widetilde{V}}(x, Q^2) = 0$$

$$g_L^{\widetilde{V}}(x, Q^2) = 0$$

$$\widetilde{V} = \gamma\gamma, \gamma Z, ZZ, \gamma \times (0), \gamma \times (1), Z \times (0), Z \times (1)$$

NC DIS cross sections in structure-function formalism:

$$\frac{d^2\sigma^{\ell}_{\mathrm{NC}}}{dx\ dQ^2} = \frac{2\pi\alpha^2}{xQ^4}\{[1+(1-y)^2]2xF_1^{\mathrm{NC}} + \mathrm{sgn}(\ell)[1-(1-y)^2]xF_3^{\mathrm{NC}} + (1-y)2F_L^{\mathrm{NC}}\}$$

$$\frac{d^2\Delta\sigma^{\ell}_{\mathrm{NC}}}{dx\ dQ^2} = \frac{8\pi\alpha^2}{xQ^4}\{[1+(1-y)^2]xg_5^{\mathrm{NC}} - \mathrm{sgn}(\ell)[1-(1-y)^2]xg_1^{\mathrm{NC}} + (1-y)g_L^{\mathrm{NC}}\}$$

Reduced cross sections:

$$\frac{d^2\sigma^{\ell}_{r,\mathrm{NC}}}{dx\ dQ^2} = \left\{\frac{4\pi\alpha^2}{xQ^4}[1+(1-y)^2]\right\}^{-1}\frac{d^2\sigma^{\ell}_{\mathrm{NC}}}{dx\ dQ^2}$$

$$\frac{d^2\Delta\sigma^{\ell}_{r,\mathrm{NC}}}{dx\ dQ^2} = \left\{\frac{4\pi\alpha^2}{xQ^4}[1+(1-y)^2]\right\}^{-1}\frac{d^2\Delta\sigma^{\ell}_{\mathrm{NC}}}{dx\ dQ^2}$$

From here on, *cross section* means *reduced cross section*.

DIS cross section at NLO QCD

Feynman diagrams describing NLO QCD corrections at parton level for the process $\ell + H \to \ell' + X$:

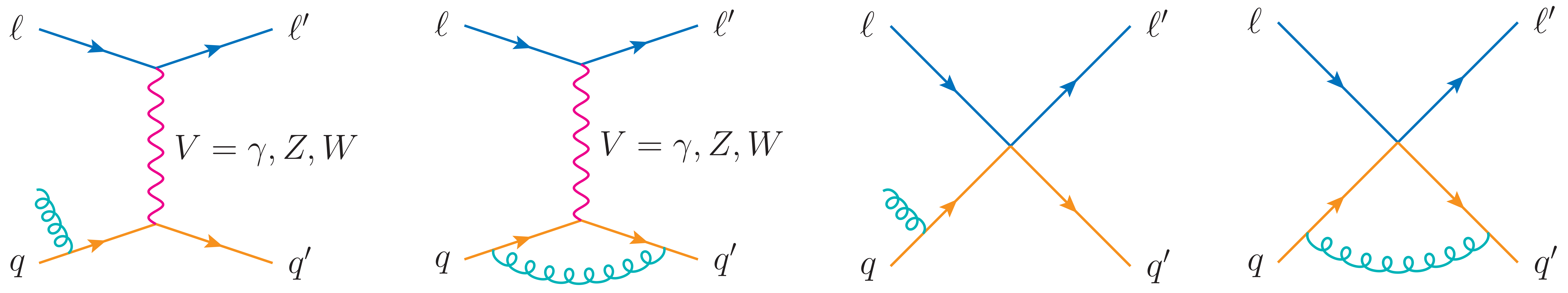

NLO QCD corrections take place only along the quark line $\Rightarrow$ identical corrections to both SM and SMEFT structure functions. These corrections are well known [de Florian *et al.* 1210.7203].

SMEFT NLO structure functions:

$$F_1^{\widetilde{V}} = \frac{1}{2}\sum_q \lambda_V^{\widetilde{V}}\left[q + \frac{\alpha_s}{2\pi}\left(\widetilde{C}_{q_1}\otimes q + \widetilde{C}_{g_1}\otimes g\right)\right]$$

$$F_3^{\widetilde{V}} = \sum_q - \operatorname{sgn}(q)\lambda_A^{\widetilde{V}}\left[q + \frac{\alpha_s}{2\pi}\left(\widetilde{C}_{q_3}\otimes q + \widetilde{C}_{g_3}\otimes g\right)\right]$$

$$F_L^{\widetilde{V}} = x\sum_q \operatorname{sgn}(q)\lambda_V^{\widetilde{V}}\left[0 + \frac{\alpha_s}{2\pi}\left(\widetilde{C}_{q_L}\otimes q + \widetilde{C}_{g_L}\otimes g\right)\right]$$

$$g_1^{\widetilde{V}} = \frac{1}{2}\sum_q \lambda_V^{\widetilde{V}}\left[\Delta q + \frac{\alpha_s}{2\pi}\left(\widetilde{\Delta C}_{q_1}\otimes \Delta q + \widetilde{\Delta C}_{g_1}\otimes g\right)\right]$$

$$g_5^{\widetilde{V}} = \frac{1}{2}\sum_q \operatorname{sgn}(q)\lambda_A^{\widetilde{V}}\left[\Delta q + \frac{\alpha_s}{2\pi}\left(\widetilde{\Delta C}_{q_3}\otimes \Delta q + \widetilde{\Delta C}_{g_3}\otimes \Delta g\right)\right]$$

$$g_L^{\widetilde{V}} = \frac{1}{2}\sum_q \operatorname{sgn}(q)\lambda_A^{\widetilde{V}}\left[0 + \frac{\alpha_s}{2\pi}\left(\widetilde{\Delta C}_{q_L}\otimes \Delta q + \widetilde{\Delta C}_{g_L}\otimes \Delta g\right)\right]$$

PVDIS asymmetries to NLO QCD

Parity-violating DIS asymmetries in cross sections at the EIC:

- Lepton left-right asymmetries of unpolarized hadrons:

$$A^{\ell}_{\mathrm{PV}} = \frac{\sigma^{+} - \sigma^{-}}{\sigma^{+} + \sigma^{-}}$$

- Hadron left-right asymmetries with unpolarized leptons:

$$\Delta A_{\mathrm{PV}} = \frac{\Delta\sigma^{0}}{\sigma^{0}}$$

where $\sigma^{\pm} = \left.\dfrac{d^2\sigma^{\ell}_{\mathrm{NC}}}{dx\; dQ^2}\right|_{\lambda_\ell = \pm|P_\ell|}$ and $(\Delta)\sigma^{0} = \left.\dfrac{d^2(\Delta)\sigma^{\ell}_{\mathrm{NC}}}{dx\; dQ^2}\right|_{\lambda_\ell = 0}$.

Generic form of cross sections:

$$\sigma = \sigma_{\mathrm{SM}} + \sum_k C_k \, \delta\sigma_k$$

For consistency, asymmetries must be linearized:

$$A = A_{\mathrm{SM}} + \sum_k C_k \, \delta A_k$$

Data analysis

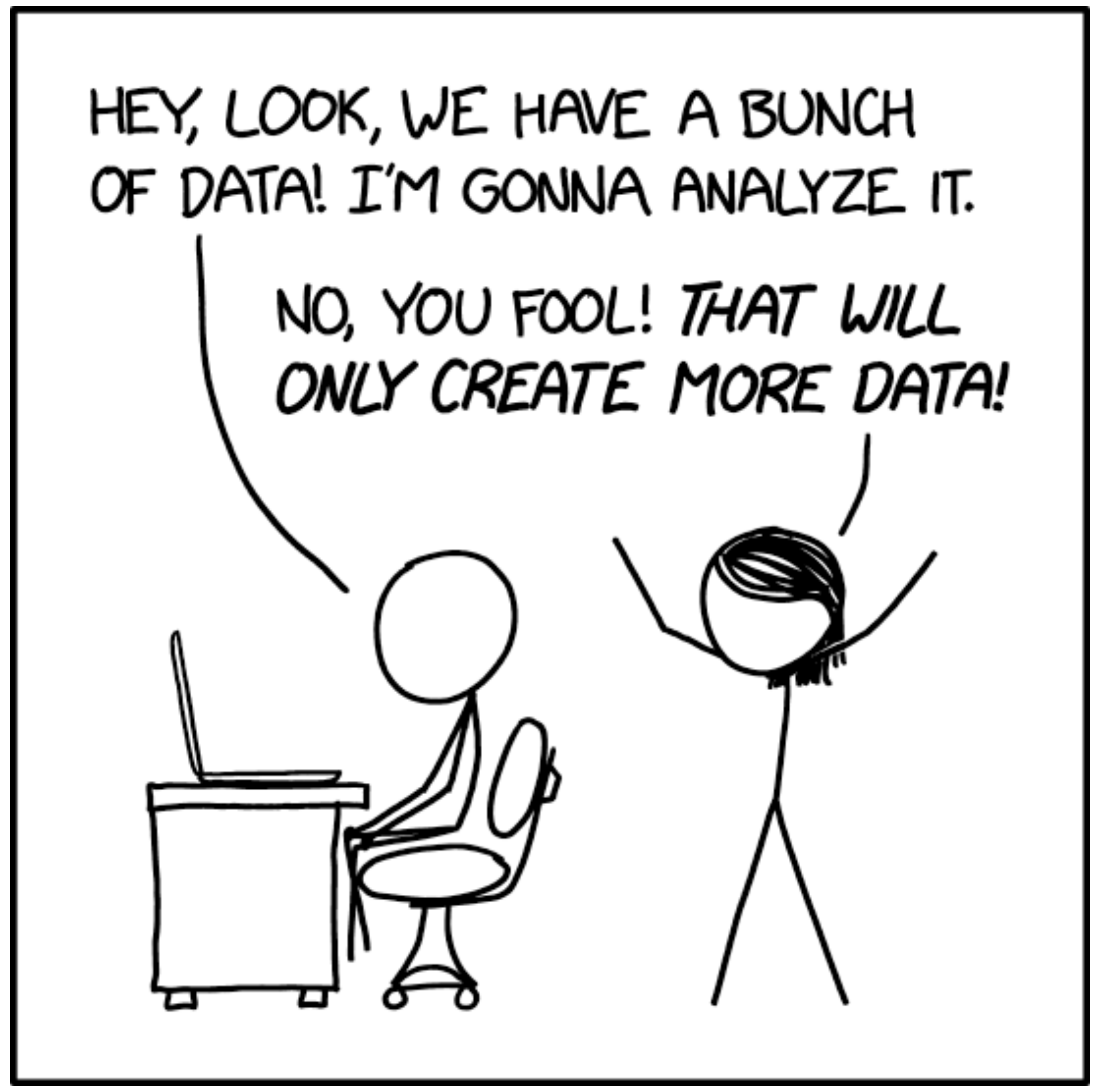

Image credit: xkcd.com

Pseudodata sets

- Most recent publicly available official LHeC pseudodata sets for NC DIS cross sections of $e^{\pm}p$ collisions [Klein (2013)].
    - The entire error matrices are given.
- Preliminary EIC data sets used in [Boughezal *et al.* 2204.07557].
    - We do not consider the 10-fold luminosity upgrade scenario at the EIC this time.

Data set label	Observable	Data set configuration
LHeC1	$\sigma_{\rm NC}$	60 GeV $\times$ 1000 GeV e^-p, $P_\ell = 0$, $\mathcal{L} = 100$ fb^{-1}
LHeC2	$\sigma_{\rm NC}$	60 GeV $\times$ 7000 GeV e^-p, $P_\ell = -80\%$, $\mathcal{L} = 100$ fb^{-1}
LHeC3	$\sigma_{\rm NC}$	60 GeV $\times$ 7000 GeV e^-p, $P_\ell = +80\%$, $\mathcal{L} = 30$ fb^{-1}
LHeC4	$\sigma_{\rm NC}$	60 GeV $\times$ 7000 GeV e^+p, $P_\ell = +80\%$, $\mathcal{L} = 10$ fb^{-1}
LHeC5	$\sigma_{\rm NC}$	60 GeV $\times$ 7000 GeV e^-p, $P_\ell = -80\%$, $\mathcal{L} = 1000$ fb^{-1}
LHeC6	$\sigma_{\rm NC}$	60 GeV $\times$ 7000 GeV e^-p, $P_\ell = +80\%$, $\mathcal{L} = 300$ fb^{-1}
LHeC7	$\sigma_{\rm NC}$	60 GeV $\times$ 7000 GeV e^+p, $P_\ell = 0$, $\mathcal{L} = 100$ fb^{-1}
(Δ)D4	$(\Delta)A_{\rm PV}$	10 GeV $\times$ 137 GeV e^-D, $\lvert P_\ell\rvert = 80\%$, $\mathcal{L} = 100$ fb^{-1}
(Δ)D5	$(\Delta)A_{\rm PV}$	18 GeV $\times$ 137 GeV e^-D, $\lvert P_\ell\rvert = 80\%$, $\mathcal{L} = 15.4$ fb^{-1}
(Δ)P4	$(\Delta)A_{\rm PV}$	10 GeV $\times$ 275 GeV e^-p, $\lvert P_\ell\rvert = 80\%$, $\mathcal{L} = 100$ fb^{-1}
(Δ)P5	$(\Delta)A_{\rm PV}$	18 GeV $\times$ 275 GeV e^-p, $\lvert P_\ell\rvert = 80\%$, $\mathcal{L} = 15.4$ fb^{-1}

Restrict ourselves to the bins with

$$x \leq 0.5$$

$$Q \geq 10 \text{ GeV}$$

$$0.1 \leq y \leq 0.9$$

to avoid large uncertainties nonperturbative QCD and nuclear dynamics occurring at low Q and high x.

Call them the *good* bins.

Kinematic coverage of the LHeC and EIC data sets:

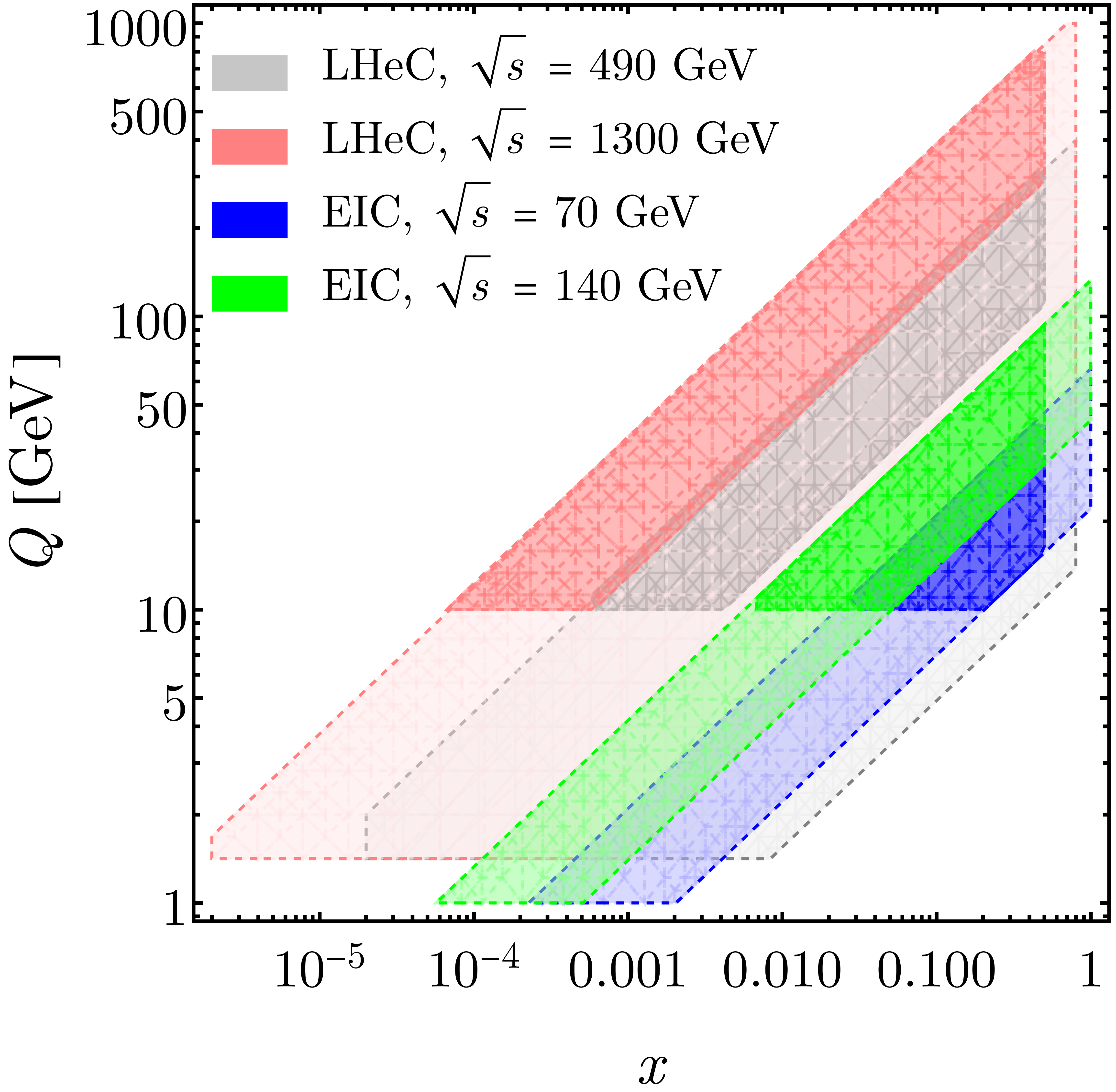

Darker regions are *good* regions considered in our analysis.

$$0.1 \leq y = \frac{Q^2}{xs} \leq 0.9$$

Lowest and highest CM energies are shown.

Anticipated uncertainties:

LHeC:

- statistical, $\delta\sigma_{\text{stat}}$
- uncorrelated efficiency, $\delta\sigma_{\text{ueff}}$
- full correlated systematics, $\delta\sigma_{\text{sys}}$:
  - lepton energy scale, $\delta\sigma_{\text{len}}$
  - lepton polar angle, $\delta\sigma_{\text{lpol}}$
  - hadron energy scale, $\delta\sigma_{\text{hen}}$
  - radiative corrections, $\delta\sigma_{\text{rad}}$
  - photoproduction, $\delta\sigma_{\text{gam}}$
  - global efficiency, $\delta\sigma_{\text{geff}}$
  - luminosity, $\delta\sigma_{\text{lum}}$, assumed 1 % rel. in σ_{NC}

EIC:

- statistical,

$$\delta A_{\text{stat}} = \frac{1}{|P_\ell|}\frac{1}{\sqrt{N}}, \quad \delta\Delta A_{\text{stat}} = \frac{|P_\ell|}{|P_H|}\frac{1}{\sqrt{N}}$$

- uncorrelated systematics, $\delta\sigma_{\text{sys}}$, assumed 1 % rel. in A_{PV}
- fully correlated beam polarization, δA_{pol}, assumed 1 % for lepton beam, 2 % for hadron beam, rel. in A_{PV}

Assume $|P_\ell| = 80\,\%$ and $|P_H| = 70\,\%$.

Fully correlated PDF uncertainties, $\delta\sigma_{\text{pdf}}$ and δA_{pdf}, are considered, as well.

Size and rank of various uncertainty components going into the diagonal entries of the error matrix for the *good* bins:

- **Stat** uncertainties are better controlled at the LHeC, constitute a minuscule part of total uncertainties. They are the leading source of errors for unpolarized asymmetries at the EIC.
- Other uncorrelated uncertainties compete with systematics and PDF errors at the LHeC. Systematics are among the lowest sources of errors at the EIC.
- Systematics, correlated at the LHeC, forms the largest source of errors at the LHeC. Correlated errors, due to beam polarization, are a tiny part of total uncertainties at the EIC.

Numerical analysis

Numerical input:

- Input scheme: $\{G_F, \alpha, M_Z\}$
- Number of active quark flavors, $N_f = 5$
- UV cut-off scale: $\Lambda = 1\ \text{TeV}$
- PDF sets: NNPDF3.1 NLO, NNPDFPOL1.1
- 2-loop running $\alpha_s(Q^2)$

Fitting procedure:

1. Form the error matrix (experimental + PDF).
2. Write down a χ^2 function.
3. Minimize it and derive the covariance matrix of fitted parameters.

Construction of the experimental error matrix:

- Uncorrelated errors:

$$\delta\sigma_{\mathrm{unc},b} = \delta\sigma_{\mathrm{stat},b} \oplus \delta\sigma_{\mathrm{ueff},b}, \qquad \delta A_{\mathrm{unc},b} = \delta A_{\mathrm{stat},b} \oplus \delta A_{\mathrm{sys},b} \qquad \text{at } b^{\mathrm{th}} \text{ bin}$$

- Correlated errors:

$$\delta\sigma_{\mathrm{cor},b} = \delta\sigma_{\mathrm{len},b} \oplus \delta\sigma_{\mathrm{lpol},b} \oplus \delta\sigma_{\mathrm{hen},b} \oplus \delta\sigma_{\mathrm{rad},b} \oplus \delta\sigma_{\mathrm{gam},b} \oplus \delta\sigma_{\mathrm{geff},b} \oplus \delta\sigma_{\mathrm{cal},b} \oplus \delta\sigma_{\mathrm{lum},b}$$

$$\delta A_{\mathrm{cor},b} = \delta A_{\mathrm{pol},b}$$

- Matrix elements:

$$E_{\mathrm{exp},bb'} = \begin{cases} (\delta Q_{\mathrm{unc}} \oplus \delta Q_{\mathrm{cor}})^2_{bb'}, & b = b' \\ \rho_{bb'}\, \delta Q_{\mathrm{cor},b}\, \delta Q_{\mathrm{cor},b'}, & b \neq b' \end{cases} \qquad Q = \sigma, A\text{: observable}$$

where we assume full correlations among bins, $\rho_{bb'} = 1$.

Construction of the PDF error matrix:

$$E_{\mathrm{pdf},bb'} = \frac{1}{N_{\mathrm{pdf}}} \sum_{m=1}^{N_{\mathrm{pdf}}} (Q_{m,b} - Q_{0,b})(Q_{m,b'} - Q_{0,b'})$$

where $Q_{0(m),b}$ is the observable evaluated at the central (m^{th}) member of the PDF set at the b^{th} bin and $N_{\mathrm{pdf}} = 100$ is the number of replica PDF members.

Total error matrix:

$$E = E_{\text{exp}} + E_{\text{pdf}}$$

χ^2 test statistic for the e^{th} pseudoexperiment:

$$\chi_e^2 = \sum_{b,b'=1}^{N_{\text{bin}}} (Q_b^{\text{SMEFT}} - Q_{e,b}) E_{bb'}^{-1} (Q_{b'}^{\text{SMEFT}} - Q_{e,b'})$$

Pseudoexperimental observable:

$$Q_{e,b} = Q_b^{\text{SM}} + r_{e,b}\ \delta Q_{\text{unc},b} + r'_e\ \delta Q_{\text{cor},b}, \qquad r_{e,b}, r'_e \sim \mathcal{N}(0,1)$$

SMEFT fit results

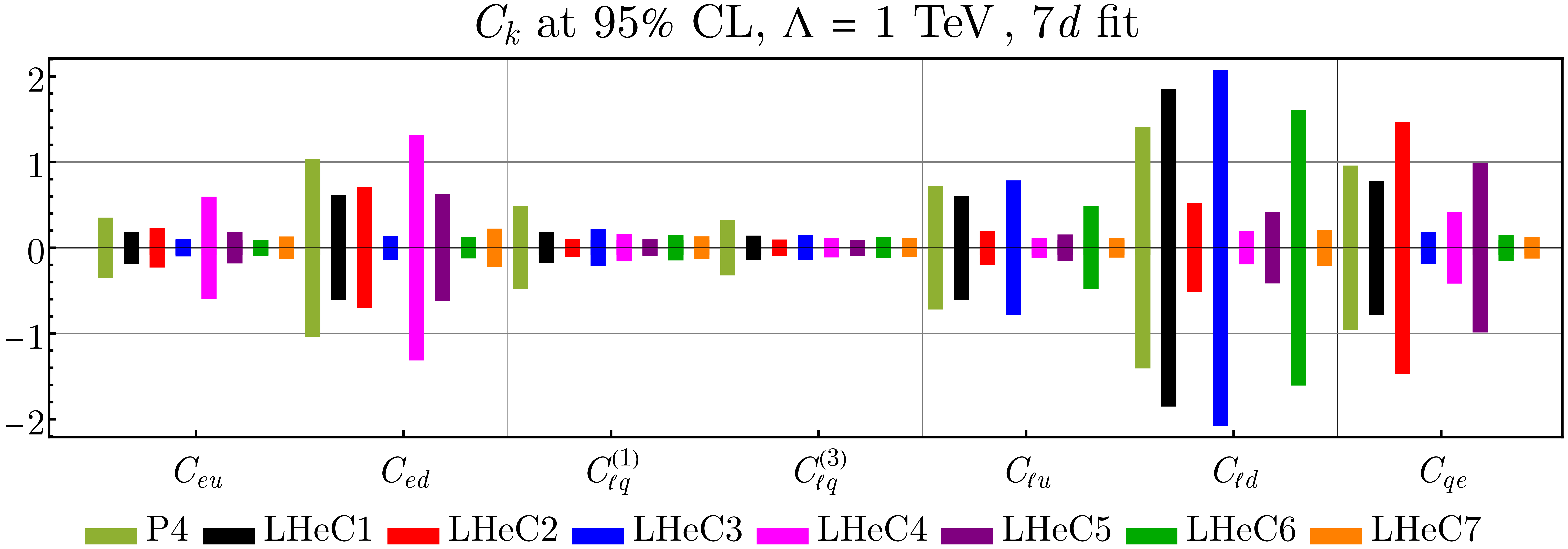

- LHeC imposes significantly stronger bounds than EIC with few exceptions. When one run yields weaker bounds, the others make up for it.
- Low-luminosity e^-p collisions with RH electrons (LHeC3 and LHeC6) provide the optimal configuration for C_{eu} and C_{ed}.
- High-luminosity e^-p collisions with LH electrons (LHeC2 and LHeC5) is the optimal configuration for $C_{\ell q}^{(1)}$ and $C_{\ell q}^{(3)}$.
- e^+p collisions (LHeC4 and LHeC7) yield the optimal configuration for $C_{\ell u}$ and $C_{\ell d}$.
- e^+p collisions with unpolarized positrons (LHeC7) serve as the optimal configuration for C_{qe}.
- No single LHeC run seems to be the *best* configuration to constrain all semi-leptonic 4-fermion Wilson coefficients.

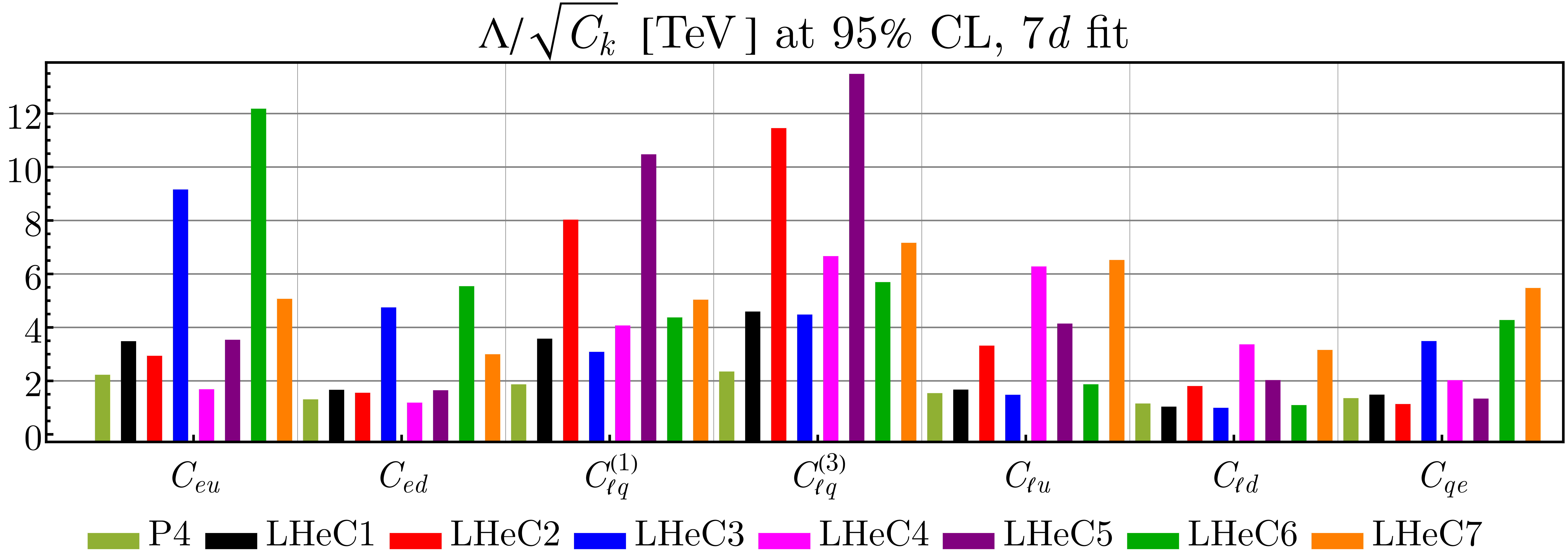

- EIC can probe UV scales up to 2 TeV, and does so with its *strongest* data set, P4.
- A large subset of LHeC runs can go beyond 5 TeV.
- Only few LHeC runs can exceed 10 TeV at 95% CL.

Strongest EIC and two *strongest* LHeC:

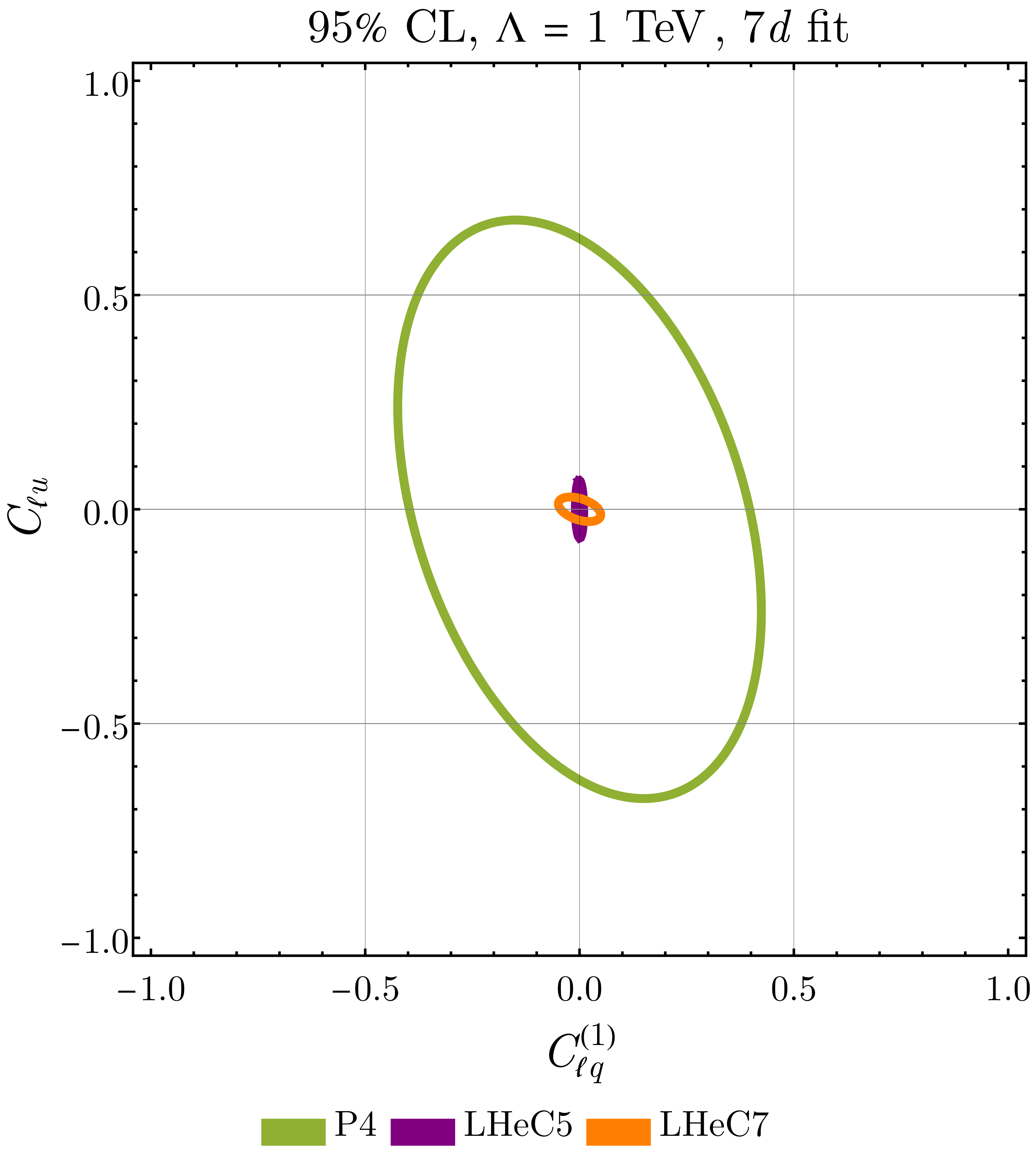

- The LHeC runs are significantly more constraining than the EIC.
- These data sets exhibit distinct correlations, complementary to each other.
- Even the two *strongest* LHeC runs can yield nearly orthogonal correlations.

Strongest EIC and two *strongest* LHeC:

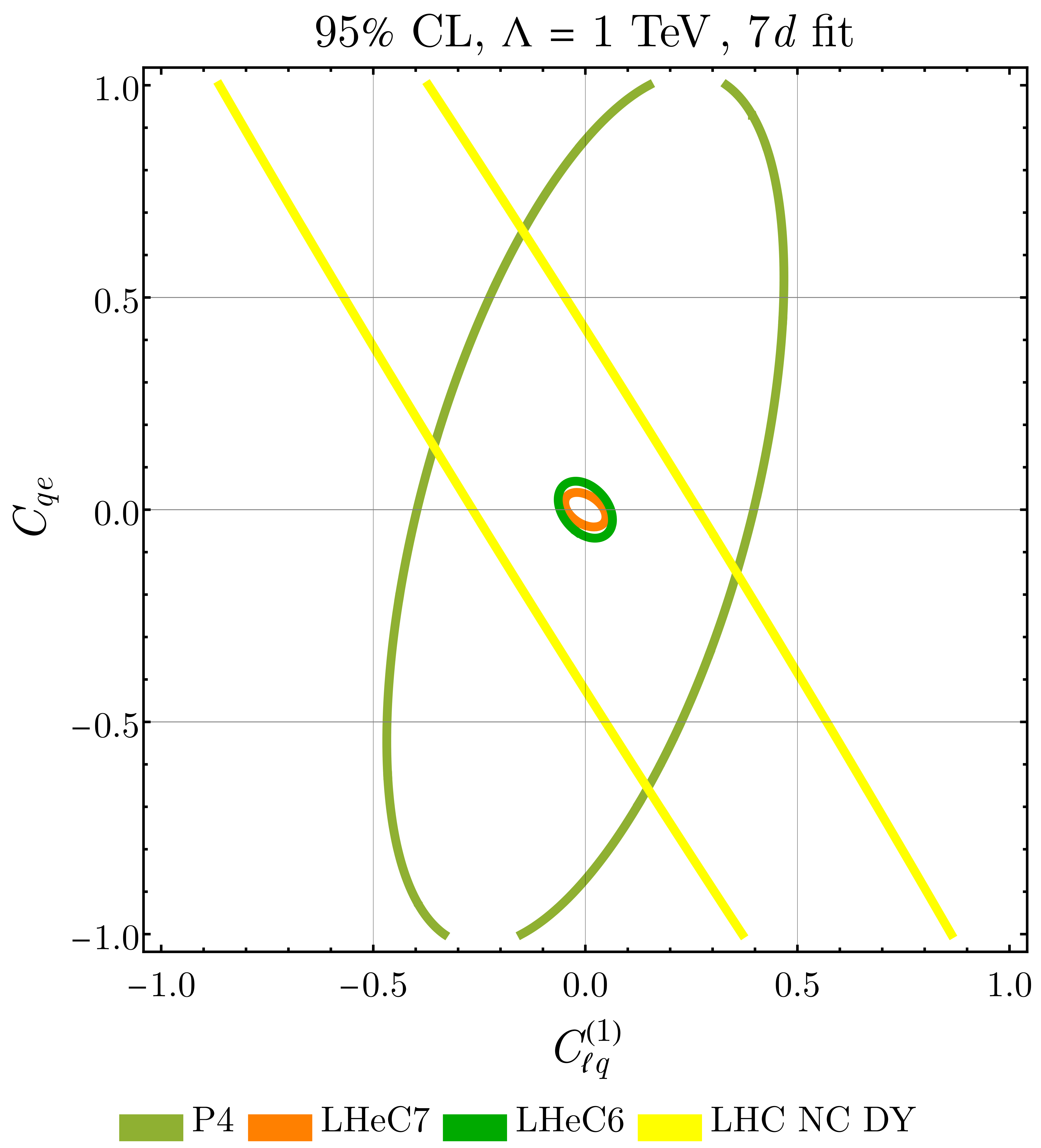

- LHC NC DY is 8 TeV 20 fb^{-1}, not 13 TeVand HL; adapted from [Boughezal *et al.* 2104.03979].
- When LHC NC DY is blind to a part of the parameter space, EIC and LHeC can resolve these blind spots, imposing strong bounds.
- LHeC fits can lead to correlations parallel to LHC NC DY, whereas EIC yields a new correlation axis.

Strongest EIC and two *strongest* LHeC:

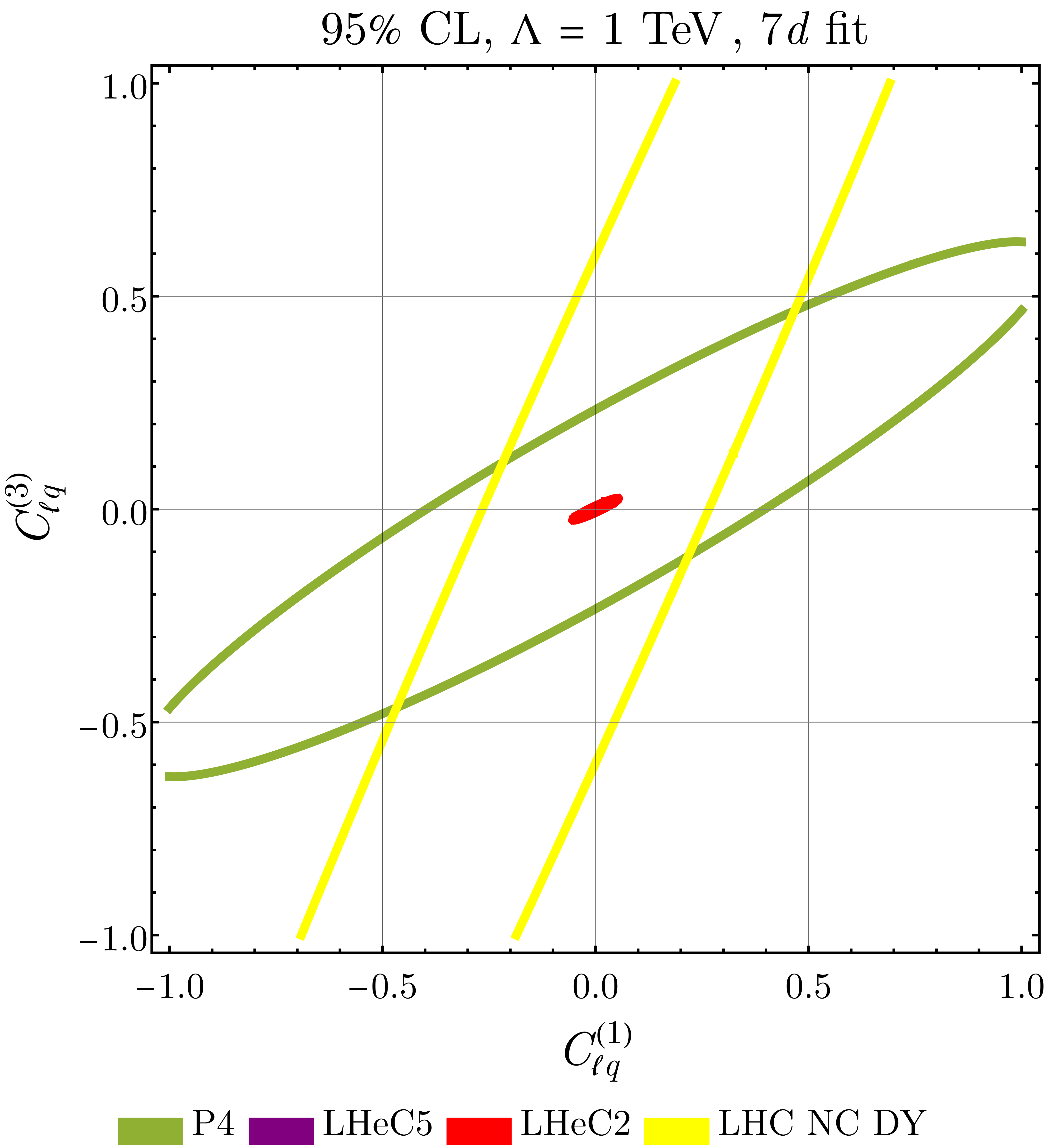

- LHC NC DY is 8 TeV 20 fb^{-1}, not 13 TeVand HL; adapted from [Boughezal *et al.* 2104.03979].
- LHC NC DY is again blind to this part of the parameter space.
- There is a slight degeneracy at the LHeC, as well.
- LHeC and EIC may yield correlations in the same directions, though in a different direction than LHC NC DY.

Data set label	Observable	Data set configuration
LHeC1	$\sigma_{\rm NC}$	60 GeV $\times$ 1000 GeV $e^-p,\ P_\ell = 0,\ \mathcal{L} = 100$ fb^{-1}
LHeC2	$\sigma_{\rm NC}$	60 GeV $\times$ 7000 GeV $e^-p,\ P_\ell = -80\%,\ \mathcal{L} = 100$ fb^{-1}
LHeC3	$\sigma_{\rm NC}$	60 GeV $\times$ 7000 GeV $e^-p,\ P_\ell = +80\%,\ \mathcal{L} = 30$ fb^{-1}
LHeC4	$\sigma_{\rm NC}$	60 GeV $\times$ 7000 GeV $e^+p,\ P_\ell = +80\%,\ \mathcal{L} = 10$ fb^{-1}
LHeC5	$\sigma_{\rm NC}$	60 GeV $\times$ 7000 GeV $e^-p,\ P_\ell = -80\%,\ \mathcal{L} = 1000$ fb^{-1}
LHeC6	$\sigma_{\rm NC}$	60 GeV $\times$ 7000 GeV $e^-p,\ P_\ell = +80\%,\ \mathcal{L} = 300$ fb^{-1}
LHeC7	$\sigma_{\rm NC}$	60 GeV $\times$ 7000 GeV $e^+p,\ P_\ell = 0,\ \mathcal{L} = 100$ fb^{-1}

Which parameter is the most important?

- Luminosity?
- Beam polarization?
- Lepton species?

- Compare LHeC2 to LHeC5 and LHeC3 to LHeC6 to check importance of luminosity.
- Compare **LHeC1** to LHeC2 to understand effects of beam polarization.
- Compare **LHeC1** to LHeC7 and LHeC3 to LHeC4 to investigate consequences of lepton species.

- Converting from low- to high-luminosity e^-p collisions can improve the bounds in a noticeable manner; however, the improvements are not sharp.

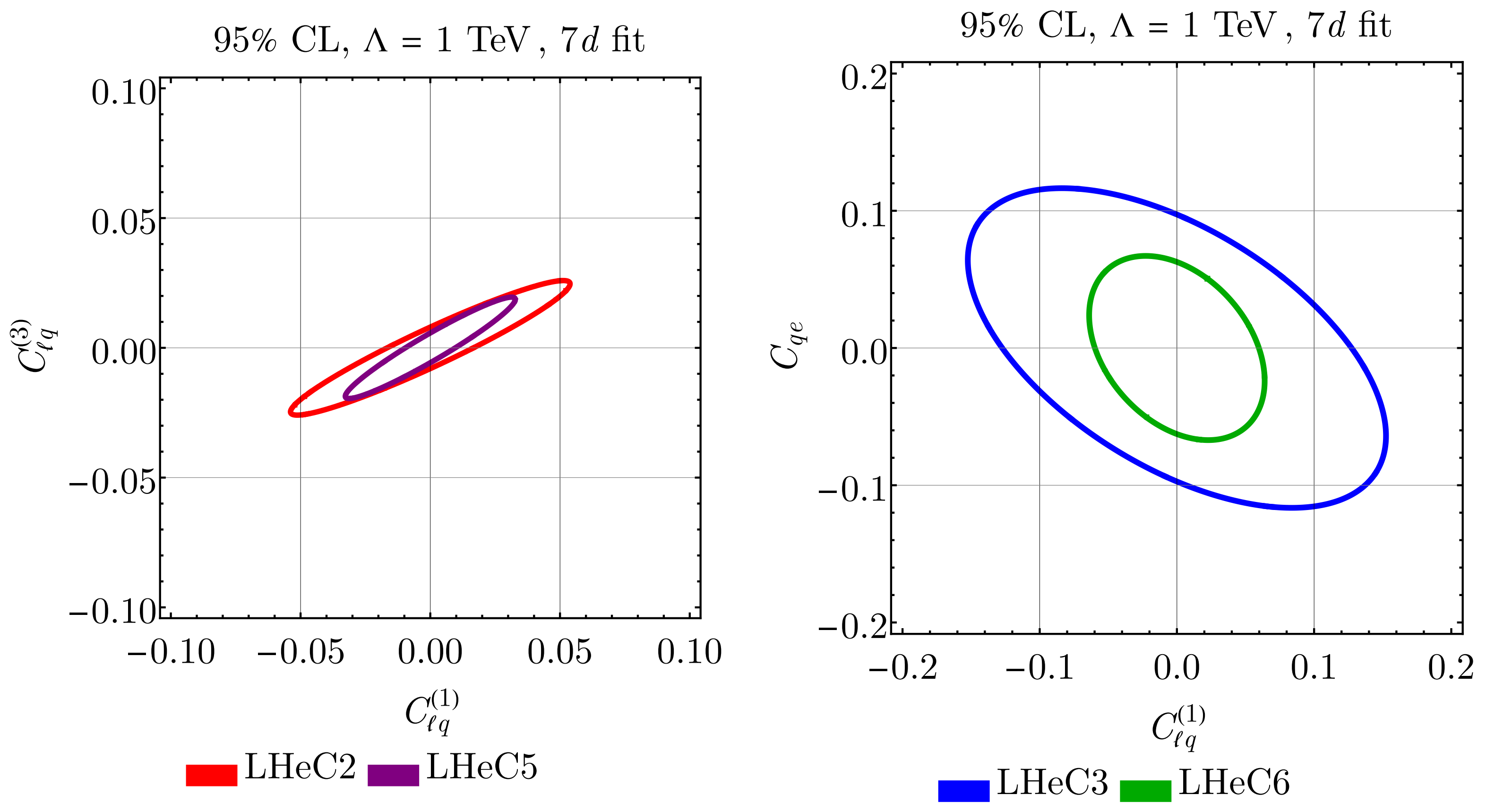

Luminosity increase:
2 to 5 and 3 to 6

LHeC2: $60\ \text{GeV} \times 7000\ \text{GeV}\ e^-p,\ P_\ell = -80\,\%\,,\ \mathscr{L} = 100\ \text{fb}^{-1}$

LHeC5: $60\ \text{GeV} \times 7000\ \text{GeV}\ e^-p,\ P_\ell = -80\,\%\,,\ \mathscr{L} = 1000\ \text{fb}^{-1}$

LHeC3: $60\ \text{GeV} \times 7000\ \text{GeV}\ e^-p,\ P_\ell = +80\,\%\,,\ \mathscr{L} = 30\ \text{fb}^{-1}$

LHeC6: $60\ \text{GeV} \times 7000\ \text{GeV}\ e^-p,\ P_\ell = +80\,\%\,,\ \mathscr{L} = 300\ \text{fb}^{-1}$

- Converting from low- to high-luminosity $e^{-}p$ collisions can improve the bounds in a noticeable manner; however, the improvements are not sharp.

- Shifting from unpolarized to LH electrons can lead to more distinguishable improvements than increasing luminosity.

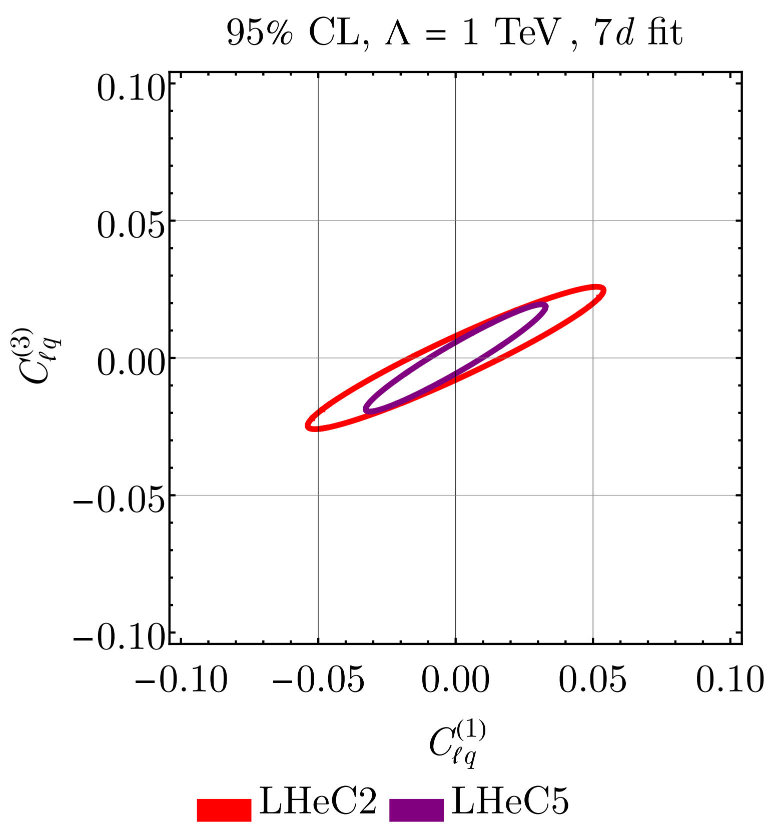

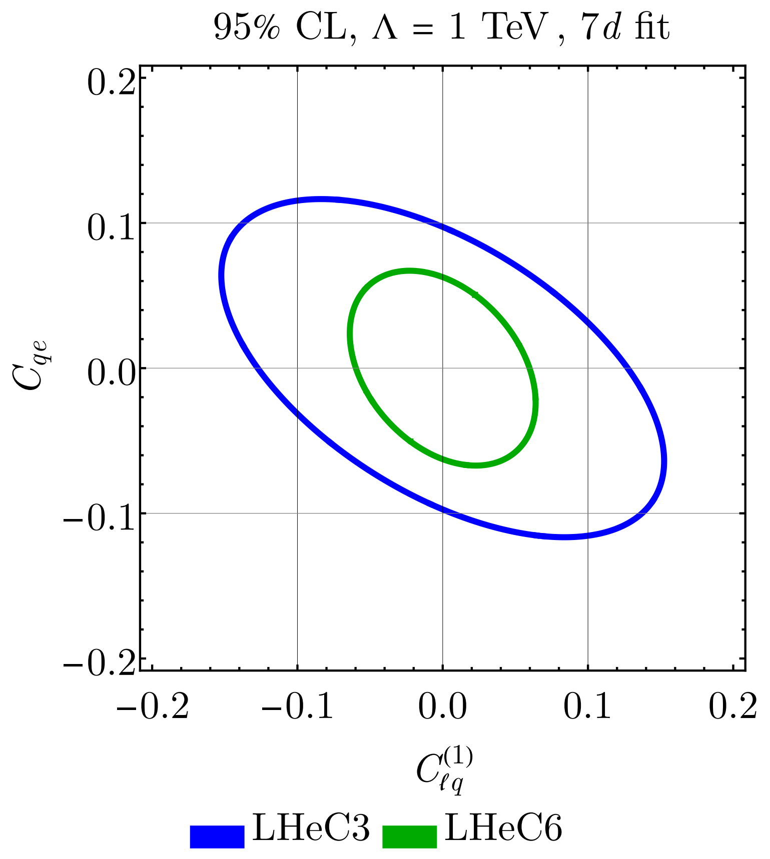

Luminosity increase:
2 to 5 and 3 to 6

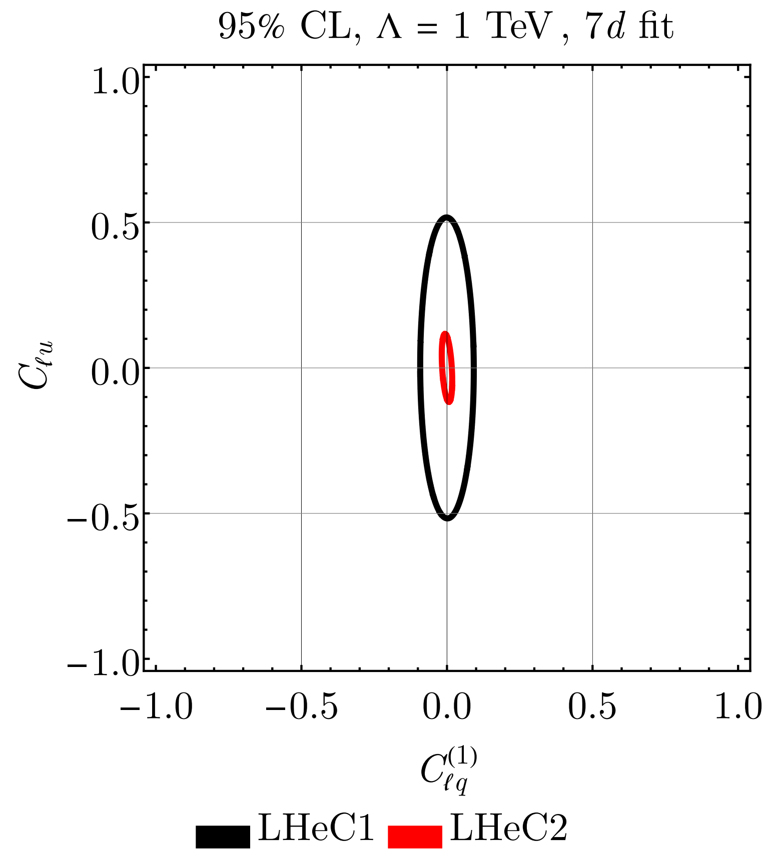

Beam polarized from unpolarized to LH e^{-}:
1 to 2

LHeC1: $60\ \text{GeV} \times 1000\ \text{GeV}\ e^{-}p,\ P_{\ell} = 0\,\%\,,\ \mathscr{L} = 100\ \text{fb}^{-1}$

LHeC2: $60\ \text{GeV} \times 7000\ \text{GeV}\ e^{-}p,\ P_{\ell} = -\,80\,\%\,,\ \mathscr{L} = 100\ \text{fb}^{-1}$

- Converting from low- to high-luminosity e^-p collisions can improve the bounds in a noticeable manner; however, the improvements are not sharp.

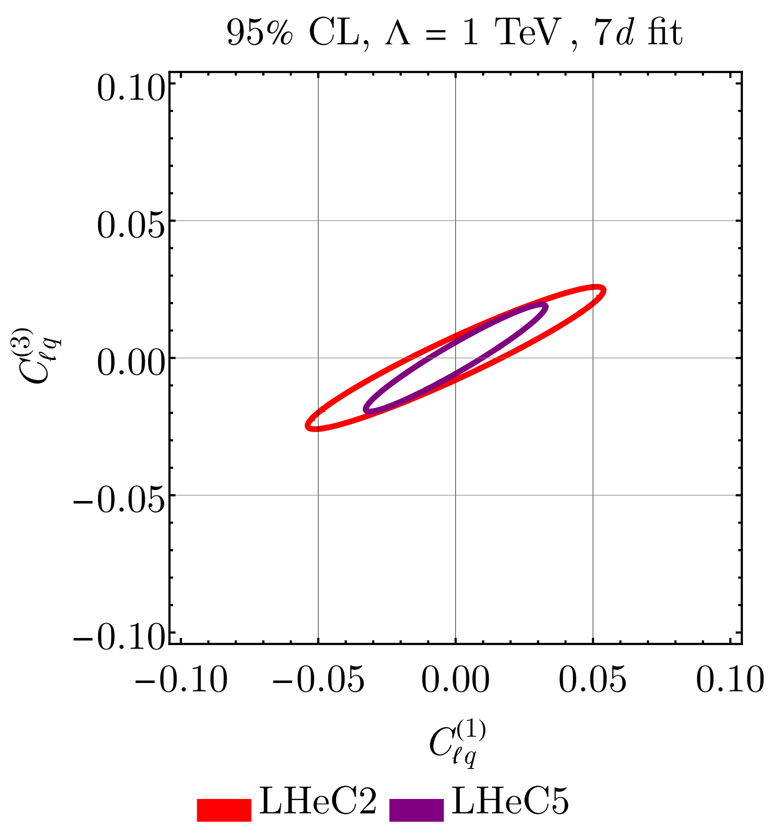

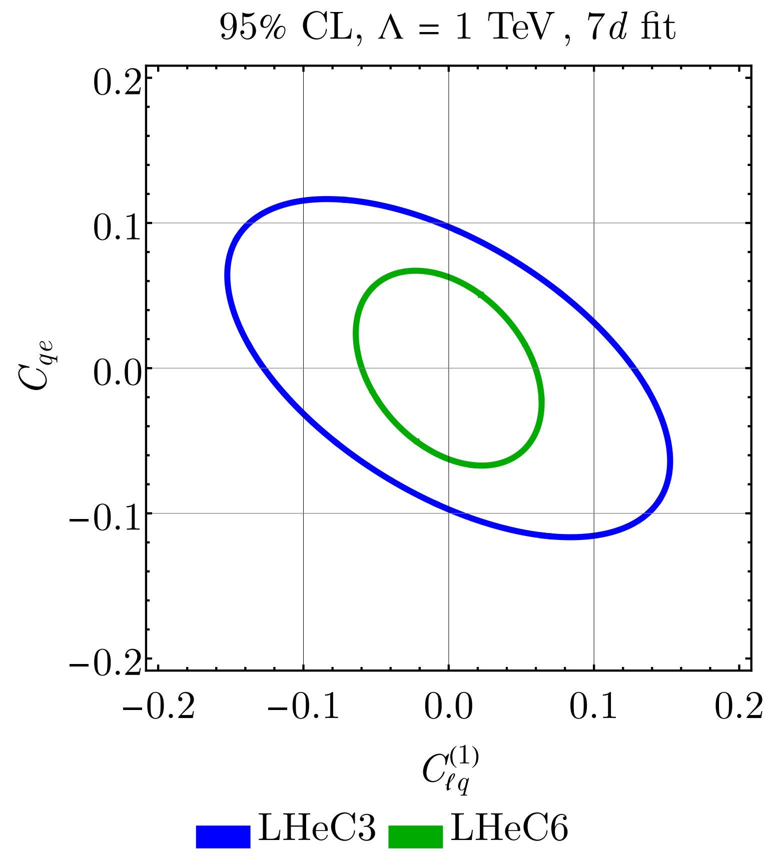

Luminosity increase:
2 to 5 and 3 to 6

- Shifting from unpolarized to LH electrons can lead to more distinguishable improvements than increasing luminosity.

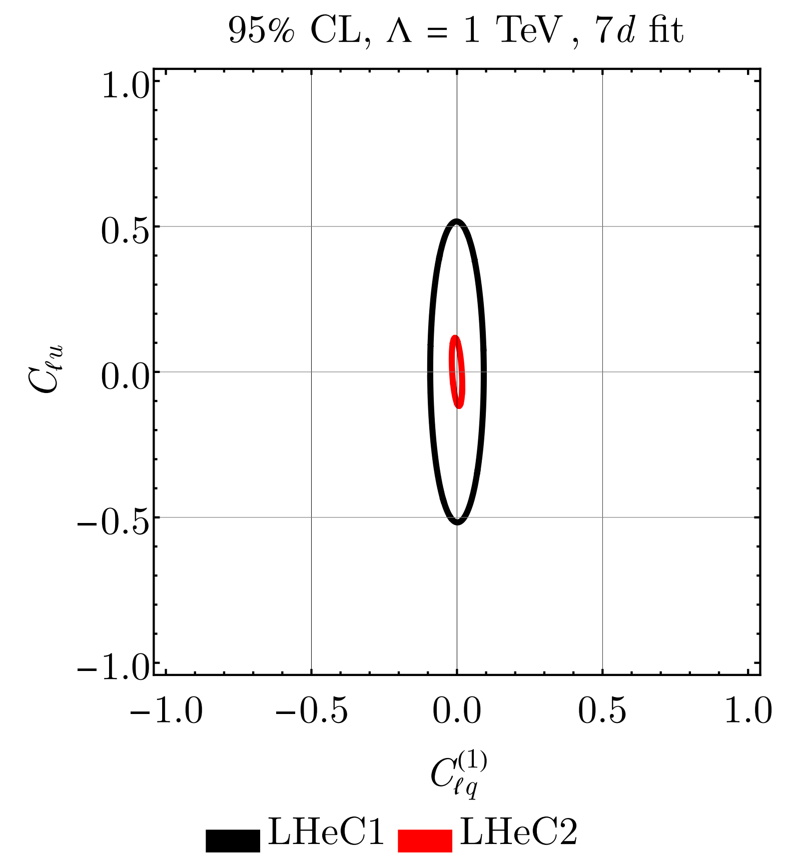

Beam polarized from
Unpolarized to LH e^-:
1 to 2

- The most drastic improvements on the bounds occur when we change lepton species from electrons to positrons.

LHeC1: 60 GeV $\times$ 1000 GeV e^-p, $P_\ell = 0\,\%$, $\mathscr{L}$ = 100 fb^{-1}
LHeC7: 60 GeV $\times$ 7000 GeV e^+p, $P_\ell = 0\,\%$, $\mathscr{L}$ = 100 fb^{-1}
LHeC3: 60 GeV $\times$ 7000 GeV e^-p, $P_\ell = +\,80\,\%$, $\mathscr{L}$ = 10 fb^{-1}
LHeC4: 60 GeV $\times$ 7000 GeV e^+p, $P_\ell = +\,80\,\%$, $\mathscr{L}$ = 10 fb^{-1}

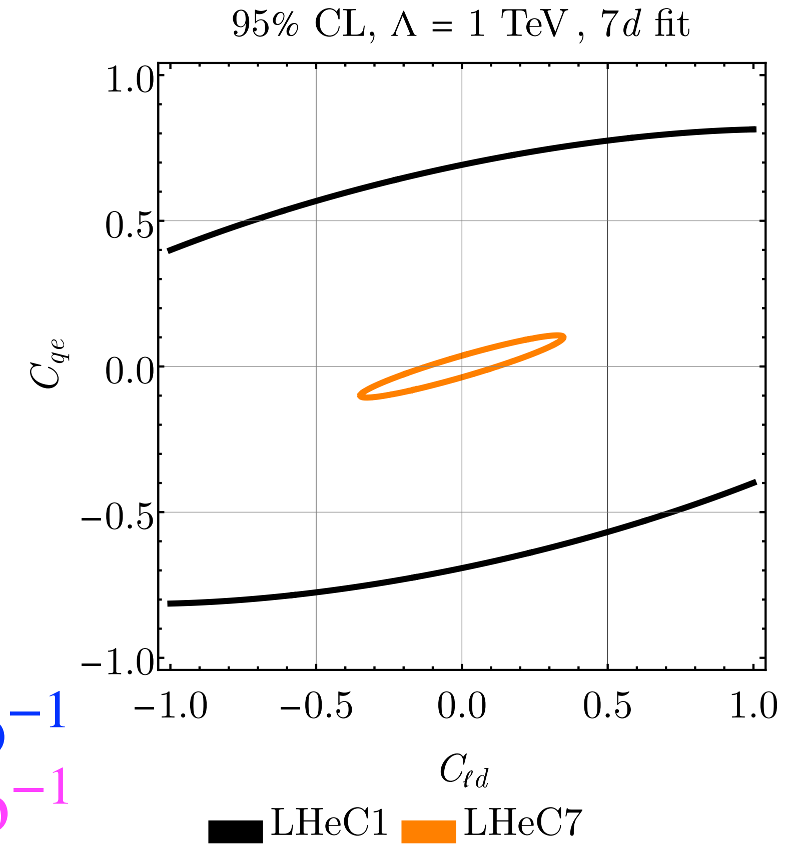

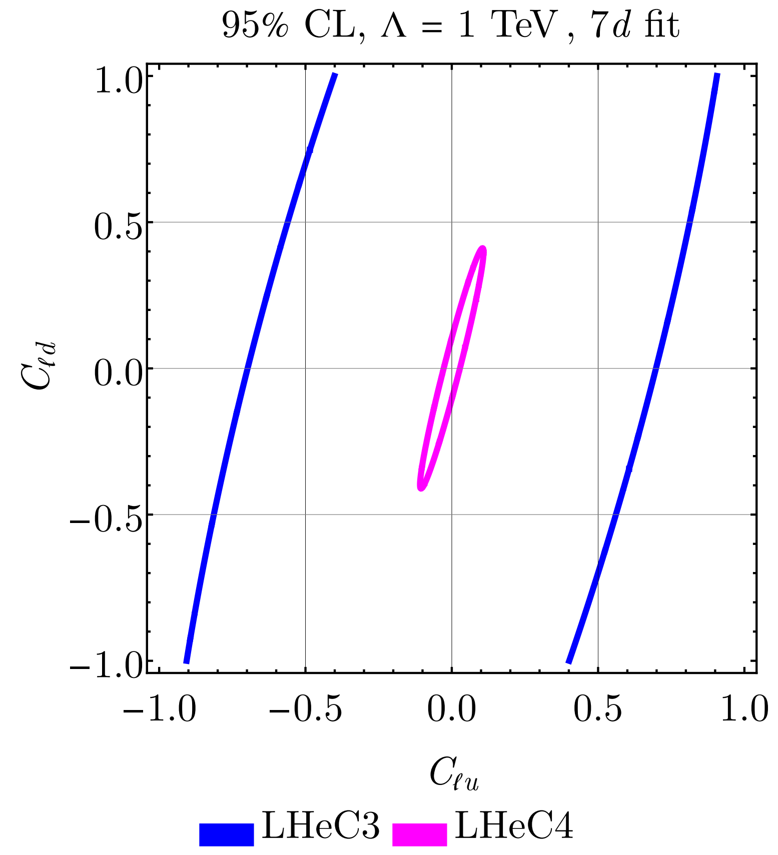

Lepton species
from e^- to e^+:
1 to 7 and 3 to 4

Joint LHeC run

- Join all 7 LHeC runs with nontrivial correlations.
- We assume only a subset of correlated uncertainties of individual data sets are correlated between runs:
  - lepton energy scale and polar angle, hadron energy scale, radiative corrections, global efficiency, calorimetry noise, luminosity, and PDF errors
  - photoproduction is excluded because said background consists of different events for each run; therefore, if we run an experiment multiple times, number of background events fluctuates without any correlations.

χ^2 function for the n^{th} run: $\chi^2_n = (\text{LHeC}n)\left(E_n\right)^{-1}(\text{LHeC}n)$

χ^2 function for the joint run: $\chi^2 = (\text{LHeC1} \quad \cdots \quad \text{LHeC7})\begin{pmatrix} E_1 & \cdots & J_{17} \\ \vdots & \ddots & \vdots \\ J_{71} & \cdots & E_7 \end{pmatrix}^{-1}\begin{pmatrix} \text{LHeC1} \\ \vdots \\ \text{LHeC7} \end{pmatrix}$

where

$$J_{nn'} = J_{\text{exp},nn'} + J_{\text{pdf},nn'}$$

$$J_{\text{exp},nn',bb'} = \rho_{nn',bb'}\,\widetilde{\delta\sigma}_{n,\text{cor},b}\,\widetilde{\delta\sigma}_{n',\text{cor},b'}, \quad \rho_{nn',bb'} = 1$$

$$J_{\text{pdf},nn',bb'} = \frac{1}{N_{\text{pdf}}}\sum_{m=1}^{N_{\text{pdf}}}(\sigma_{n,m,b} - \sigma_{n,0,b})(\sigma_{n',m,b'} - \sigma_{n',0,b'})$$

with $\widetilde{\delta\sigma}_{n,\text{cor},b}$ the same as for a single run defined before but with photoproduction errors removed.

Strongest EIC, *strongest* and *weakest* LHeC, and the joint LHeC for each Wilson coefficient:

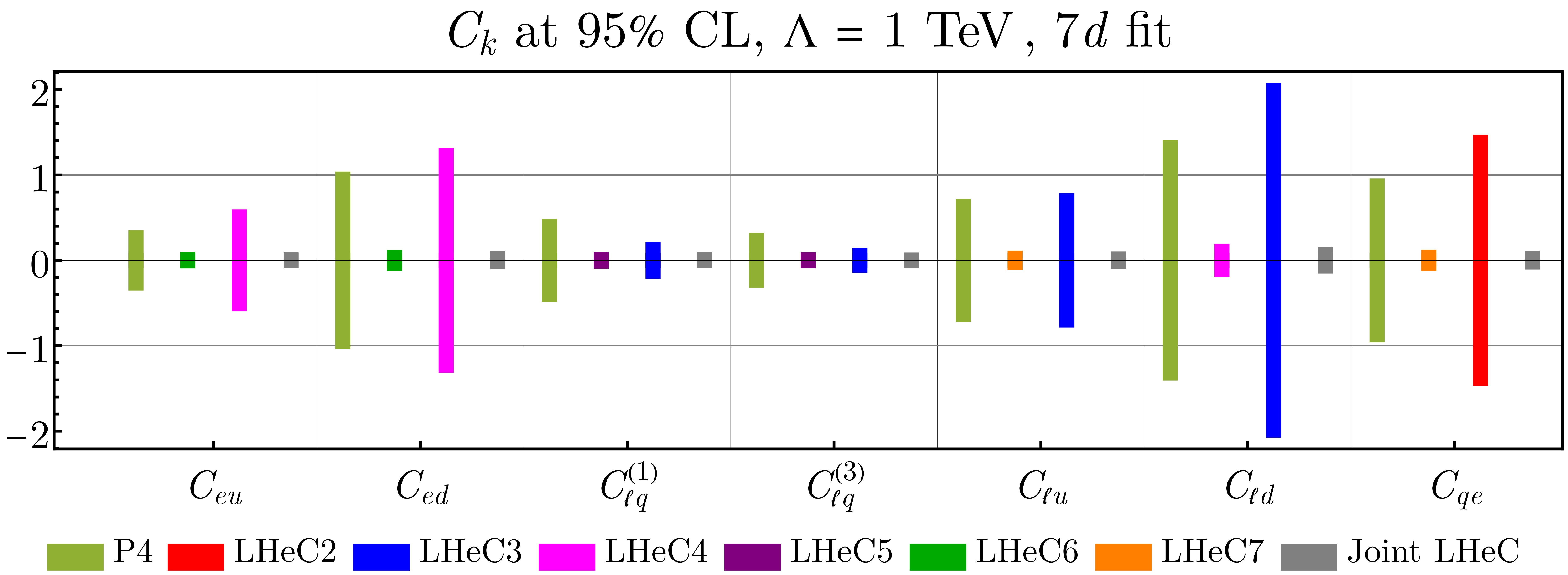

- Allowed bound from the joint run is significantly more restricting than the *weakest* LHeC set for any Wilson coefficient.
- Nonetheless, it is comparable to the *strongest* LHeC data set.

Strongest EIC, *strongest* and *weakest* LHeC, and the joint LHeC for each Wilson coefficient:

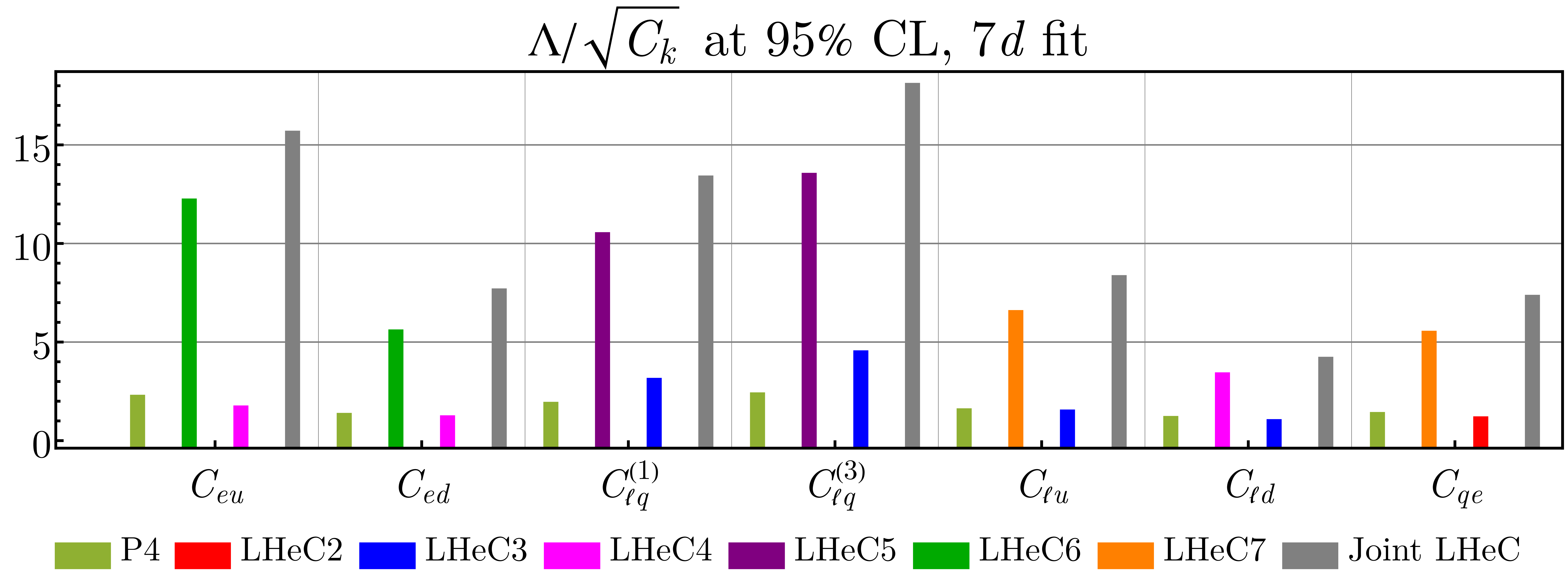

- UV scales present a clearer picture of comparison.
- In a joint run, the LHeC can probe UV scales beyond 15 TeV.
- Compared to the *strongest* LHeC run, UV scales that can be probed get deeper by 20 to 30%.

Two *strongest* LHeC sets and the joint fit for double Wilson coefficient:

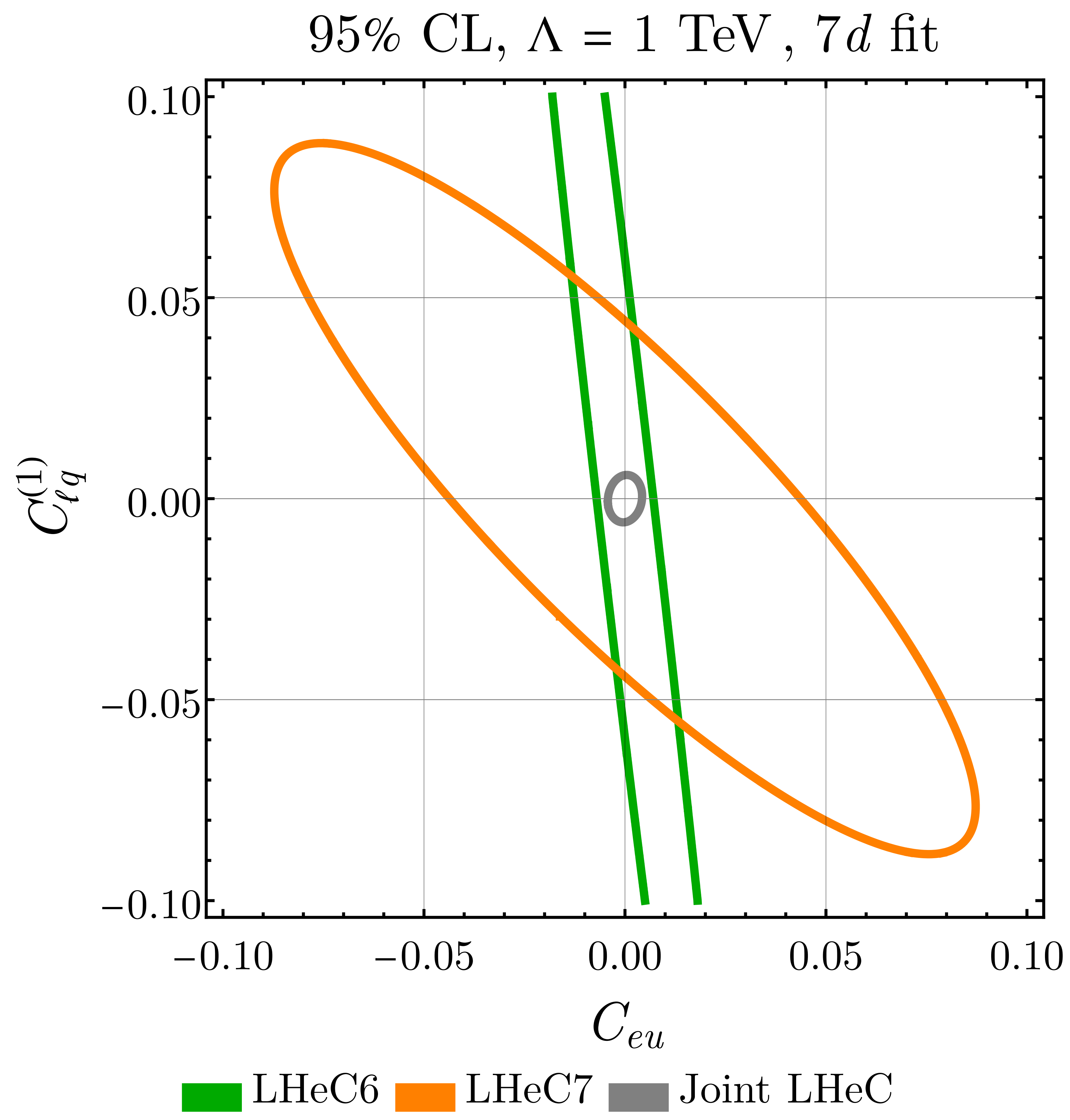

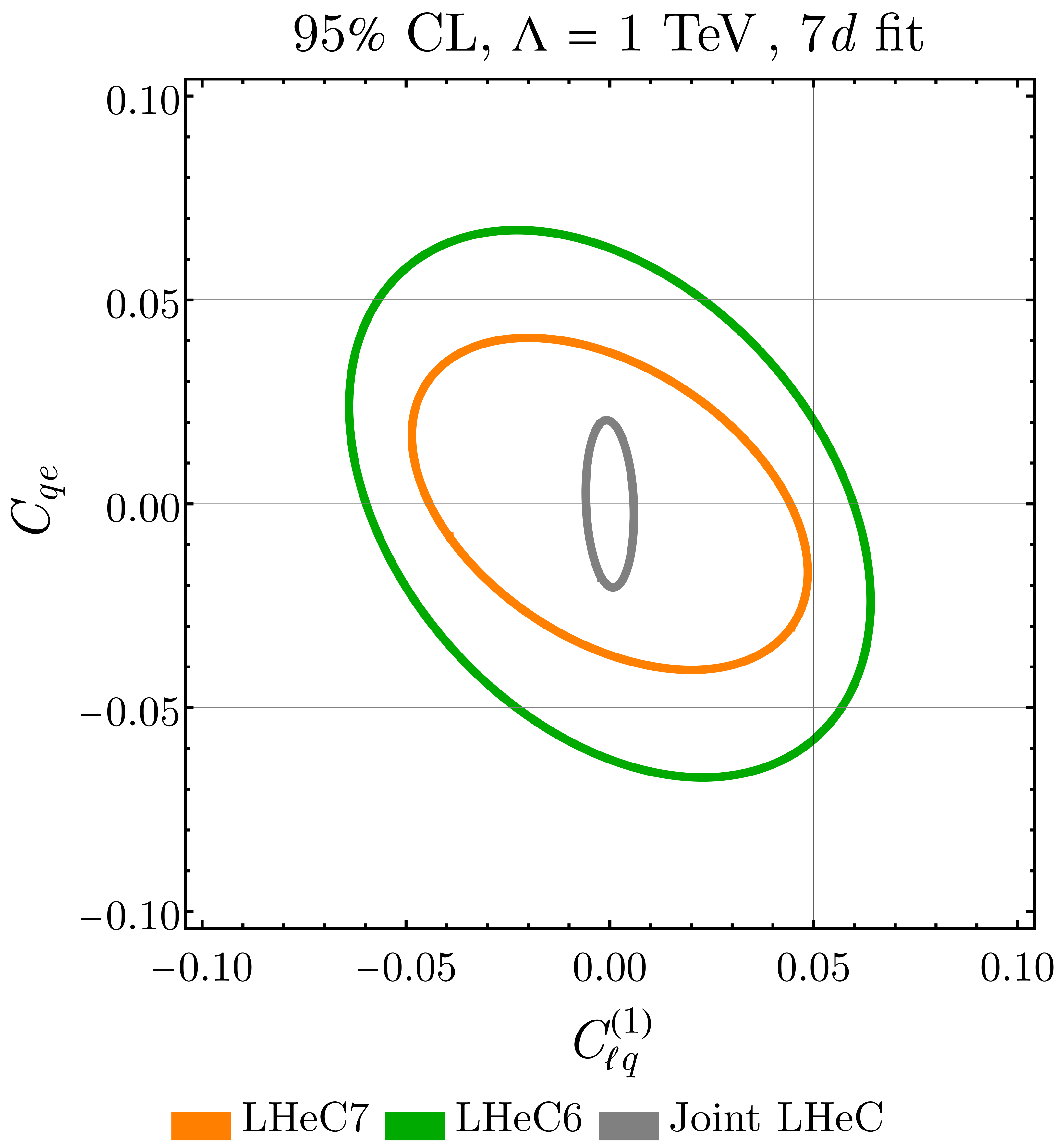

- The joint fit seems to offer bounds just comparable to the *strongest* LHeC run in $1d$ parameter subspaces. Its real power emerges in $2d$ parameter subspaces.
- Constraints are highly restricting and correlations are different than those of the two strongest LHeC sets.

Two *strongest* LHeC sets and the joint fit for double Wilson coefficients:

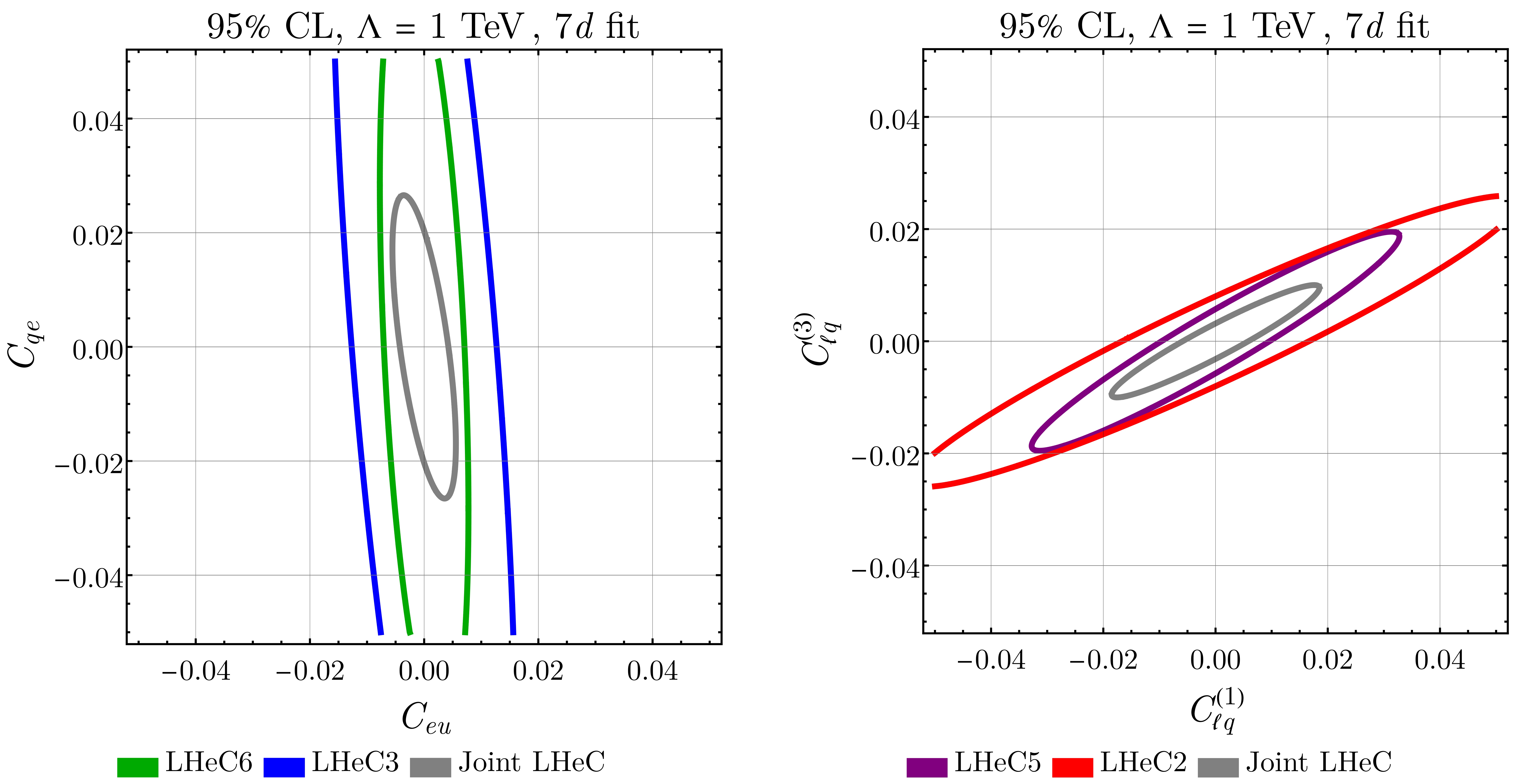

- The joint fit still offers considerably stronger bounds.
- It may not always yield remarkably distinct correlations than the individual runs.

Flat-direction analysis

SMEFT part of unpolarized hadronic cross section:

$$\frac{d^2\sigma_{\ell H}(\lambda_\ell)}{dx\ dQ^2} \supset \sum_q \frac{1}{2}\left[\frac{d^2\sigma_{\ell q}^{\gamma\times+Z\times}(\lambda_\ell,\lambda_H=1)}{dx\ dQ^2}+\frac{d^2\sigma_{\ell q}^{\gamma\times+Z\times}(\lambda_\ell,\lambda_H=-1)}{dx\ dQ^2}\right] f_{q/H}$$

Set SMEFT contributions equal to zero to investigate blind spots.

Two structures, 1 and $(1-y)^2$, and two types of quarks, u_i and d_i $\Rightarrow$ four equations $\Rightarrow$ number of *free* Wilson coefficients becomes $7-4=3$.

We focus on four different bases spanned by free Wilson coefficients:

- Basis 1: $\{C_{\ell q}^{(1)}, C_{\ell q}^{(3)}, C_{qe}\}$ $\Rightarrow$ all LH quarks
- Basis 2: $\{C_{eu}, C_{ed}, C_{qe}\}$ $\Rightarrow$ all RH leptons
- Basis 3: $\{C_{\ell q}^{(1)}, C_{\ell q}^{(3)}, C_{\ell u}\}$ $\Rightarrow$ all LH leptons with a focus on the up-quark channel
- Basis 4: $\{C_{\ell q}^{(1)}, C_{\ell q}^{(3)}, C_{\ell d}\}$$\Rightarrow$ all LH leptons with a focus on the down-quark channel

Examples to flat-direction relations:

$$\text{Basis 1:}(C_{\ell q}^{(1)}, C_{\ell q}^{(3)}, C_{qe}) \begin{cases} C_{eu} = \dfrac{P_\ell - 1}{P_\ell + 1} \dfrac{Q_u - g_+^e g_+^u \eta_\gamma \eta_Z}{Q_u - g_-^e g_-^u \eta_\gamma \eta_Z} (C_{\ell q}^{(1)} - C_{\ell q}^{(3)}) \\ C_{\ell u} = \dfrac{P_\ell + 1}{P_\ell - 1} \dfrac{Q_u - g_-^e g_+^u \eta_\gamma \eta_Z}{Q_u - g_-^u g_+^e \eta_\gamma \eta_Z} C_{qe} \\ C_{ed} = \dfrac{P_\ell - 1}{P_\ell + 1} \dfrac{Q_d - g_+^d g_+^e \eta_\gamma \eta_Z}{Q_d - g_-^d g_-^e \eta_\gamma \eta_Z} (C_{\ell q}^{(1)} + C_{\ell q}^{(3)}) \\ C_{\ell d} = \dfrac{P_\ell + 1}{P_\ell - 1} \dfrac{Q_d - g_-^e g_+^d \eta_\gamma \eta_Z}{Q_d - g_-^d g_+^e \eta_\gamma \eta_Z} C_{qe} \end{cases}$$

$$\text{Basis 3:}(C_{\ell q}^{(1)}, C_{\ell q}^{(3)}, C_{\ell u}) \begin{cases} C_{eu} = \dfrac{P_\ell - 1}{P_\ell + 1} \dfrac{Q_u - g_+^e g_+^u \eta_\gamma \eta_Z}{Q_u - g_-^e g_-^u \eta_\gamma \eta_Z} (C_{\ell q}^{(1)} - C_{\ell q}^{(3)}) \\ C_{ed} = \dfrac{P_\ell - 1}{P_\ell + 1} \dfrac{Q_d - g_+^d g_+^e \eta_\gamma \eta_Z}{Q_d - g_-^d g_-^e \eta_\gamma \eta_Z} (C_{\ell q}^{(1)} + C_{\ell q}^{(3)}) \\ C_{\ell d} = \dfrac{Q_d - g_-^e g_+^d \eta_\gamma \eta_Z}{Q_d - g_-^d g_+^e \eta_\gamma \eta_Z} \dfrac{g_-^u g_+^e \eta_\gamma \eta_Z - Q_u}{g_-^e g_+^u \eta_\gamma \eta_Z - Q_u} C_{\ell u} \\ C_{qe} = \dfrac{P_\ell - 1}{P_\ell + 1} \dfrac{Q_u - g_-^u g_+^e \eta_\gamma \eta_Z}{Q_u - g_-^e g_+^u \eta_\gamma \eta_Z} C_{\ell u} \end{cases}$$

Flat directions defined by these relations are only approximate due to the energy-dependent eta factors:

$$\eta_\gamma \eta_Z = \frac{G_F M_Z^2}{2\sqrt{2}\pi\alpha} \frac{Q^2}{Q^2 + M_Z^2}$$

They become exact only in the limit $Q^2/M_Z^2 \to \infty$. Thus, we assume

$$\eta_\gamma \eta_Z \approx \frac{G_F M_Z^2}{2\sqrt{2}\pi\alpha}$$

Examples to flat-direction relations:

$$\text{Basis 1:}(C_{\ell q}^{(1)}, C_{\ell q}^{(3)}, C_{qe}) \begin{cases} C_{eu} = \dfrac{P_\ell - 1}{P_\ell + 1} \dfrac{Q_u - g_+^e g_+^u \eta_\gamma \eta_Z}{Q_u - g_-^e g_-^u \eta_\gamma \eta_Z} (C_{\ell q}^{(1)} - C_{\ell q}^{(3)}) \\ C_{\ell u} = \dfrac{P_\ell + 1}{P_\ell - 1} \dfrac{Q_u - g_-^e g_+^u \eta_\gamma \eta_Z}{Q_u - g_-^u g_+^e \eta_\gamma \eta_Z} C_{qe} \\ C_{ed} = \dfrac{P_\ell - 1}{P_\ell + 1} \dfrac{Q_d - g_+^d g_+^e \eta_\gamma \eta_Z}{Q_d - g_-^d g_-^e \eta_\gamma \eta_Z} (C_{\ell q}^{(1)} + C_{\ell q}^{(3)}) \\ C_{\ell d} = \dfrac{P_\ell + 1}{P_\ell - 1} \dfrac{Q_d - g_-^e g_+^d \eta_\gamma \eta_Z}{Q_d - g_-^d g_+^e \eta_\gamma \eta_Z} C_{qe} \end{cases}$$

$$\text{Basis 3:}(C_{\ell q}^{(1)}, C_{\ell q}^{(3)}, C_{\ell u}) \begin{cases} C_{eu} = \dfrac{P_\ell - 1}{P_\ell + 1} \dfrac{Q_u - g_+^e g_+^u \eta_\gamma \eta_Z}{Q_u - g_-^e g_-^u \eta_\gamma \eta_Z} (C_{\ell q}^{(1)} - C_{\ell q}^{(3)}) \\ C_{ed} = \dfrac{P_\ell - 1}{P_\ell + 1} \dfrac{Q_d - g_+^d g_+^e \eta_\gamma \eta_Z}{Q_d - g_-^d g_-^e \eta_\gamma \eta_Z} (C_{\ell q}^{(1)} + C_{\ell q}^{(3)}) \\ C_{\ell d} = \dfrac{Q_d - g_-^e g_+^d \eta_\gamma \eta_Z}{Q_d - g_-^d g_+^e \eta_\gamma \eta_Z} \dfrac{g_-^u g_+^e \eta_\gamma \eta_Z - Q_u}{g_-^e g_+^u \eta_\gamma \eta_Z - Q_u} C_{\ell u} \\ C_{qe} = \dfrac{P_\ell - 1}{P_\ell + 1} \dfrac{Q_u - g_-^u g_+^e \eta_\gamma \eta_Z}{Q_u - g_-^e g_+^u \eta_\gamma \eta_Z} C_{\ell u} \end{cases}$$

Moreover, the LHeC runs have only very specific polarization values:

- Case 1: Unpolarized leptons, $P_\ell = 0$: LHeC1 and 7
- Case 2: RH/LH electrons/positrons, $P_\ell = \pm 80\,\%$: LHeC2, 4, and 5
- Case 3: LH/RH electrons/positrons, $P_\ell = \mp 80\,\%$: LHeC3 and 6

Shown data sets are in each case are enforced to exhibit flat directions.

We want to see if the EIC can resolve these blind spots; therefore, we now include other EIC sets in our comparison, as well.

We indeed observe weaker constraints or diminished UV probes in the expected cases of flat directions. The good news is, other LHeC runs seem promising in resolving these blind spots; in fact, LHeC3 and LHeC6 appear highly enthusiast to in most cases.

However, the four *strongest* EIC data sets can barely compete in resolving degeneracies with LHeC runs that survive flat-direction conditions.

Extended parameter space

- Turn on Wilson coefficients in the ffV sector now.
- Purpose is to see if the LHeC can resolve the degeneracies observed the EWPO fits.
- 9 operators shifting the ffV vertices $\Rightarrow$ 16 fitted parameters now.

95 % CL bounds in single-parameter fits at $\Lambda = 1$ TeV

	Joint LHeC	Dawson's [1909.02000]	Mimasu's [2012.02779]
$C_{\varphi WB}$	$[-0.020, 0.020]$	$[-0.0088, 0.0013]$	$[-0.0043, 0.0026]$
$C_{\varphi D}$	$[-0.030, 0.030]$	$[-0.025, 0.0019]$	$[-0.023, 0.0027]$
$C_{\varphi \ell}^{(3)}$	$[-0.067, 0.067]$	$[-0.012, 0.0029]$	$[-0.01, 0.003]$
$C_{\varphi \ell}^{(1)}$	$[-0.067, 0.067]$	$[-0.0043, 0.012]$	$[-0.0044, 0.013]$
$C_{\varphi e}$	$[-0.11, 0.11]$	$[-0.013, 0.0094]$	$[-0.015, 0.0071]$
$C_{\varphi q}^{(3)}$	$[-0.080, 0.080]$	$[-0.011, 0.014]$	$[-0.017, 0.012]$
$C_{\varphi q}^{(1)}$	$[-0.16, 0.16]$	$[-0.027, 0.043]$	$[-0.1, 0.14]$
$C_{\varphi d}$	$[-0.22, 0.22]$	$[-0.16, 0.060]$	$[-0.13, 0.071]$
$C_{\varphi u}$	$[-0.091, 0.091]$	$[-0.072, 0.091]$	$[-0.075, 0.073]$
Comments on actual fits:	16*d* fit to joint LHeC runs	9*d* global fit to *Z* and *W* pole observables	34*d* global fit to EW, diboson, Higgs, and top data

EWPO fits better constrain the relevant Wilson coefficients in the *ffV* sector in single-parameter fits.

Shown bounds are for single Wilson coefficients activated one at a time.

Comparison of double-parameter fits:

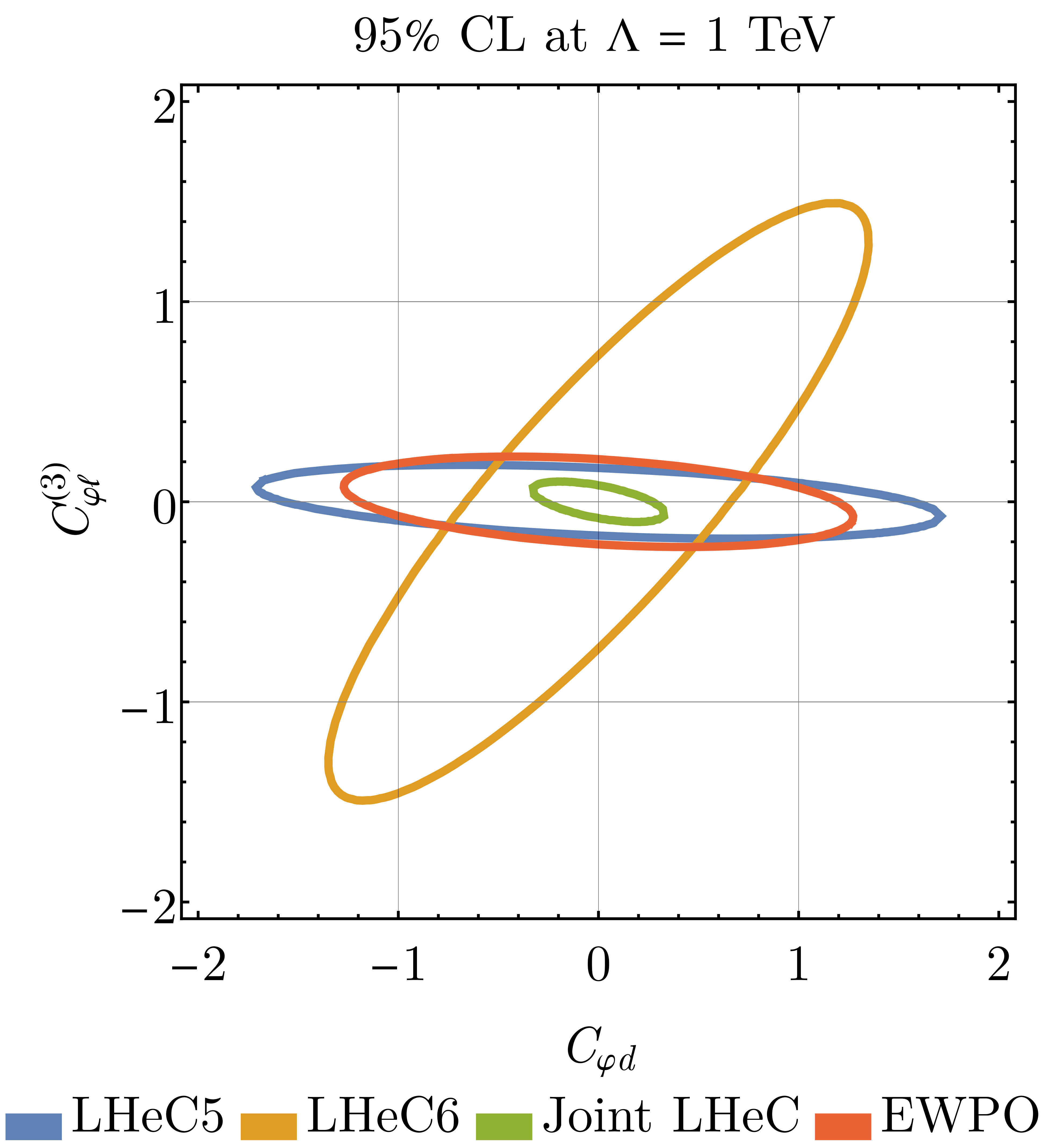

Comments:

- Shown are the non-marginalized ellipses.

(Only 2 Wilson coefficients are activated at a time.)

- EWPO fits are adapted from [Mimasu *et al.* 2012.02779].

Resolution of flat directions observed in EWPO fits:

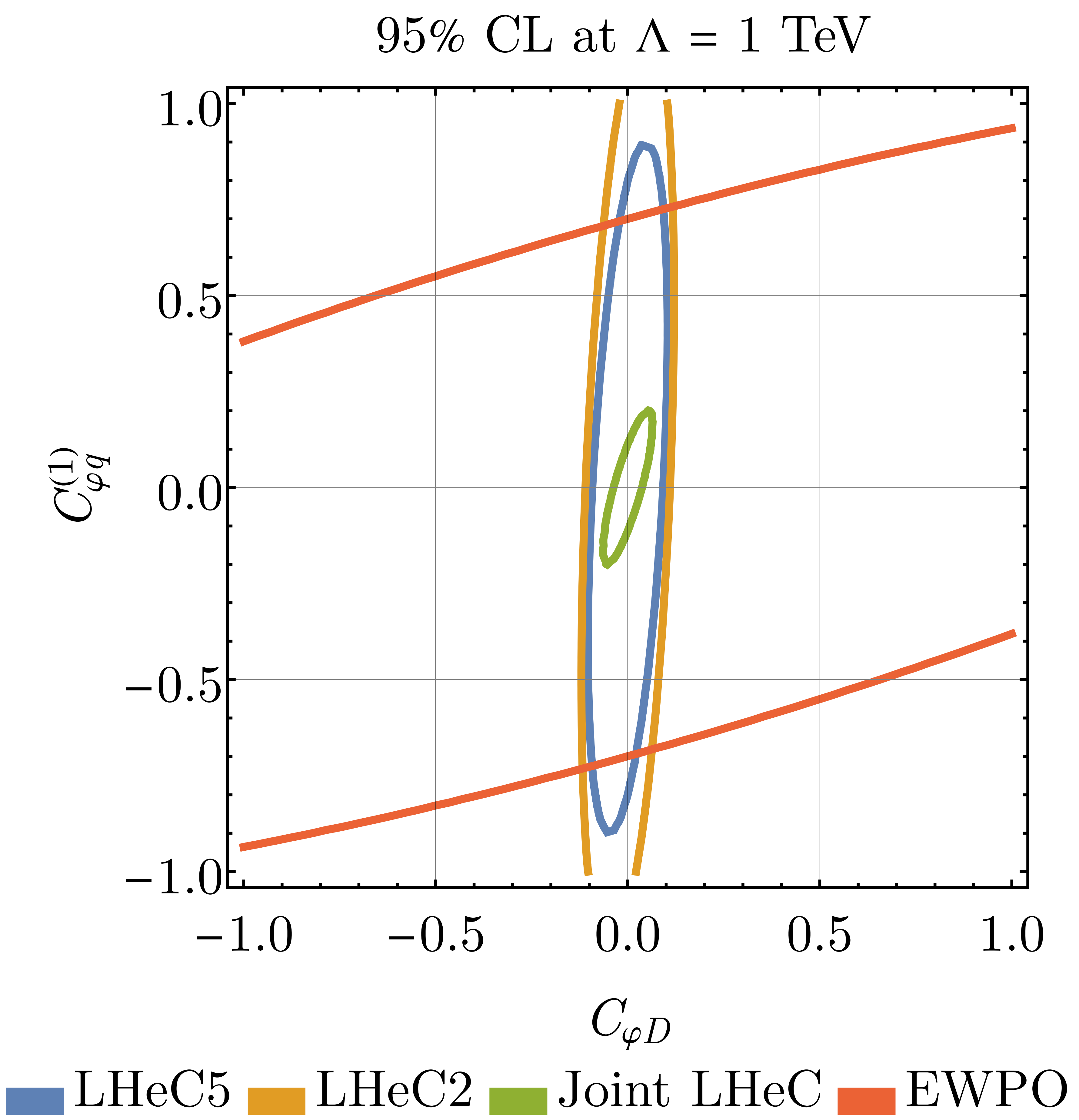

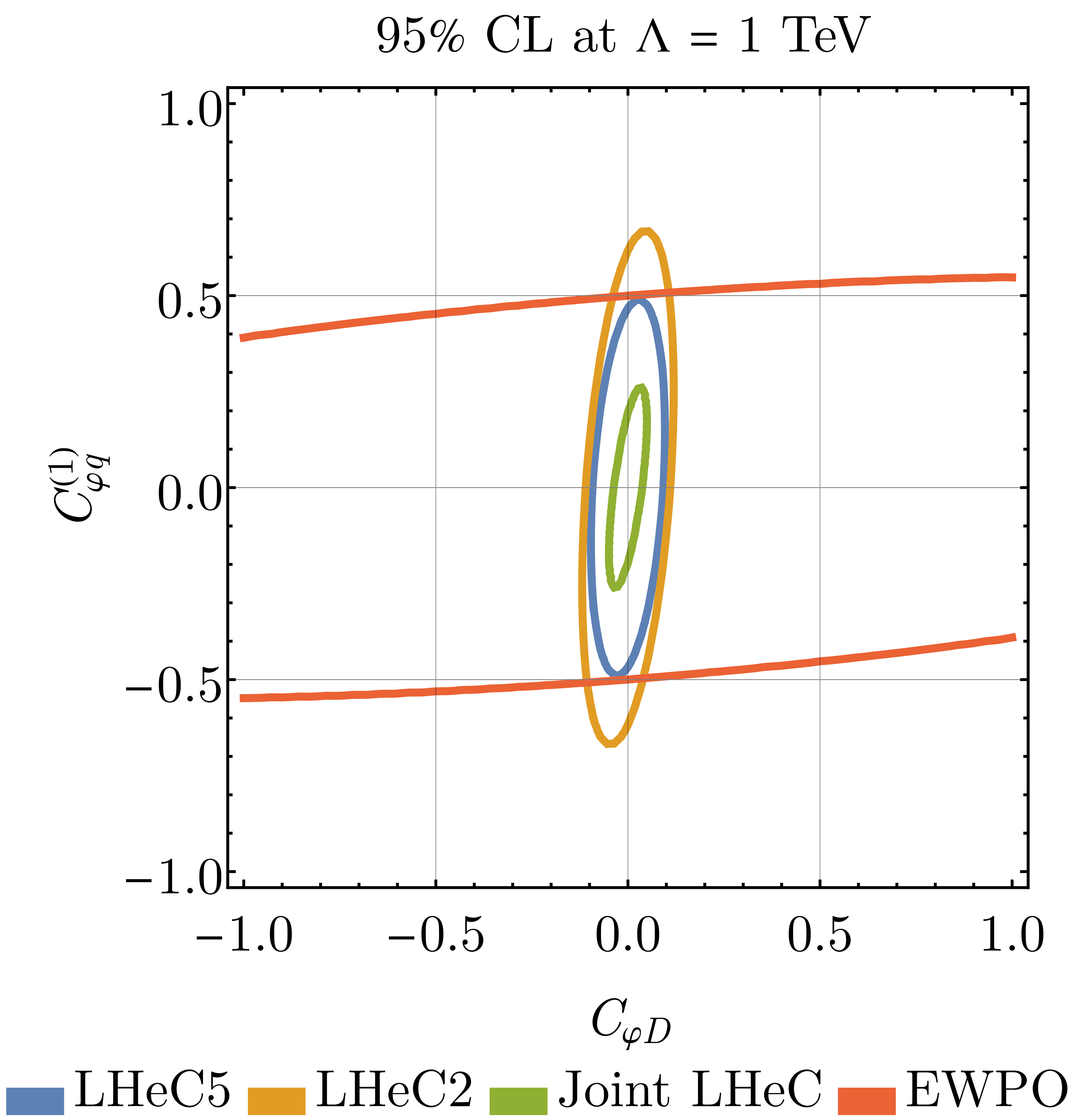

Comments:

- Shown are the non-marginalized ellipses. (Only 2 Wilson coefficients are activated at a time.)
- EWPO fits are adapted from [Mimasu *et al.* 2012.02779].

Coda

Conclusion

- We have studied the BSM potential of the EIC and LHeC to NLO QCD within the model-independent framework of the SMEFT.
- We have focused on the semi-leptonic 4-fermion operators first and then extended our parameter space to include the SMEFT ffV corrections, all at dimension 6.
- We have found that
  - the EIC can probe UV scales ~ 2 TeV and the LHeC > 10 TeV and even > 15 TeV with a joint fit;
  - the bounds from the EIC may barely compete with the ones from the LHeC; nevertheless, they lead to distinct correlations, indicating complementarity;
  - both the EIC and LHeC can strongly resolve degeneracies observed in the LHC NC Drell-Yan fits;
  - one LHeC fit may suffer from blind spots itself, but another LHeC fit or even the EIC resolves it;
  - the LHeC seems promising in resolving flat directions observed in the ffV sector in the EWPO fits.

Outlook

- Promotion of the EIC data sets to include SMEFT ffV corrections (in progress)
- Upgrade of both EIC and LHeC to include dimension-8 SMEFT operators
  - 54 operators but not all independent
  - Vertex factors already extracted
  - A possible LanHEP code to more systematically obtain Feynman rules, allowing one to channel them into FeynArts directly
- EW corrections to study HERA data
- Switching from Mathematica to a faster language and writing a comprehensive package for cross sections